ELSEVIER

www.elsevier.nl/locate/jorganchem

Journal of Organometallic Chemistry 620 (2001) 150–164

Journal of Organometallic Chemistry

Migratory insertion and CO substitution reactions of the β,γ-unsaturated esters and amides $[Fe_2(CO)_5(\mu\text{-}PPh_2)(\mu\text{-}\eta^1\text{:}\eta^2\text{-}\{NuC(O)CH_2\}C{=}CH_2\}]$ (Nu = OMe, OEt, OPr^i, NHPh, NHBu^t): synthesis and characterisation of acyl-bridged $[Fe_2(CO)_4L_2(\mu\text{-}PPh_2)(\mu\text{-}C{=}O\{C{=}CH_2\}CH_2C(O)Nu)]$ (L_2 = dppm, dppe) and alkenyl-bridged $[Fe_2(CO)_4\{P(Ome)_3\}_2(\mu\text{-}PPh_2)(\mu\text{-}\eta^1\text{:}\eta^2\text{-}\{NuC(O)CH_2\}C{=}CH_2)]$

Simon Doherty [a,*], Graeme Hogarth [b], Mark Waugh [a], Tom H. Scanlan [a],
Mark R.J. Elsegood [a], William Clegg [a]

[a] *Department of Chemistry, Bedson Building, The University of Newcastle upon Tyne, Newcastle upon Tyne NE1 7RU, UK*
[b] *Department of Chemistry, University College London, 20 Gordon Street, London WC1H 0AJ, UK*

Received 30 August 2000; received in revised form 28 September 2000; accepted 28 September 2000

This contribution is dedicated to Professor Arthur J. Carty on the occasion of his 60th birthday

Abstract

Reaction of the β,γ-unsaturated esters and amides $[Fe_2(CO)_5(\mu\text{-}PPh_2)(\mu\text{-}\eta^1(O)\text{:}\eta^1(C)\text{:}\eta^2(C)\text{-}\{NuC(O)CH_2\}C{=}CH_2)]$ (Nu = OMe, **1a**; R = OEt, **1b**; R = OPr^i, **1c**, R = NHPh, **1d**, R = NHBu^t, **1e**) with dppe and dppm results in displacement of the acyl carbonyl and migratory insertion to give the α,β,-unsaturated acyl derivatives $[Fe_2(CO)_4(\eta^2\text{-dppe})(\mu\text{-}PPh_2)(\mu\text{-}C{=}O\{C{=}CH_2\}CH_2C(O)Nu)]$ (Nu = OMe, **2a**; R = OEt, **2b**; R = OPr^i, **2c**, R = NHPh, **2d**, R = NHBu^t, **2e**) and $[Fe_2(CO)_4(\mu\text{-dppm})(\mu\text{-}PPh_2)(\mu\text{-}C{=}O\{C{=}CH_2\}CH_2C(O)Nu)]$ (R = OMe, **3a**; R = OEt, **3b**; R = OPr^i, **3c**, R = NHPh, **3d**), respectively. Single-crystal X-ray analyses of **2a** and **3a** has revealed that the dppe ligand in the former chelates, with one arm binding *trans* and one *cis* to the phosphido bridge, while the dppm and phosphido group in the latter both bridge the iron-iron bond and are *trans* to one another. In contrast, reaction of **1a**–**c** with trimethylphosphite results in displacement of the ester carbonyl oxygen to give $[Fe_2(CO)_5\{P(OMe)_3\}(\mu\text{-}PPh_2)(\mu\text{-}\eta^1(C)\text{:}\eta^2(C)\text{-}\{NuC(O)CH_2\}C{=}CH_2\}]$ (Nu = OMe, **4a**; R = OEt, **4b**; R = OPr^i, **4c**) followed by CO substitution to give $[Fe_2(CO)_4\{P(OMe)_3\}_2(\mu\text{-}PPh_2)(\mu\text{-}\eta^1(C)\text{:}\eta^2(C)\text{-}\{Nu(O)CCH_2\}C{=}CH_2)]$ (Nu = OMe, **6a**; R = OEt, **6b**; R = OPr^i, **6c**) with no evidence for the formation of the corresponding acyl-bridged derivative. Thermolysis of toluene solutions of **4a**–**c** result in loss of CO and coordination of the oxygen atom of the ester carbonyl to give $[Fe_2(CO)_4\{P(OMe)_3\}(\mu\text{-}PPh_2)(\mu\text{-}\eta^1(O)\text{:}\eta^1(C)\text{:}\eta^2(C)\text{-}\{NuC(O)CH_2\}C{=}CH_2)]$ (Nu = OMe, **5a**; R = OEt, **5b**; R = OPr^i, **5c**), an intermediate in the formation of **6a**–**c**. Complexes **5a** and **6a** have been characterised by single-crystal X-ray crystallography. © 2001 Elsevier Science B.V. All rights reserved.

Keywords: Diiron; Migratory insertion; Acyl; Diphosphine; Alkenyl; Decarbonylation; Trigonal twist

1. Introduction

Migratory insertion of carbonyl into a metal–alkyl bond is a synthetically useful transformation which is utilised in a number of important stoichiometric and catalytic reactions [1]. For instance, chiral iron enolates

---

* Corresponding author. Tel.: +44-191-2226644; fax: +44-191-2226929.
E-mail address: simon.doherty@newcastle.ac.uk (S. Doherty).

0022-328X/01/$ - see front matter © 2001 Elsevier Science B.V. All rights reserved.
PII: S0022-328X(00)00823-8

derived from the corresponding acyl compounds have been used to prepare β- and γ-lactams via complex multistep intramolecular cyclisations [2], and palladium acyl complexes are key intermediates in the synthesis of α,β-unsaturated carboxylic acids, esters amides, aldehydes and ketones, often with elaborate architectures [3]. In addition iron acyl complexes are convenient precursors to non-heteroatom and heteroatom stabilised carbene complexes [4].

The most common migratory insertion reaction is that involving carbon monoxide and a σ-bond of a mononuclear metal–alkyl or alkenyl complex [5]. Although less numerous, there has recently been an increasing number of reports of carbonyl insertion into unsaturated metal bound hydrocarbons such as σ-η-alkenyls, to generate the corresponding binuclear α,β-unsaturated acyl derivatives [6]. In contrast to the widespread use of mononuclear α,β-unsaturated acyl complexes in organic synthesis, there are surprisingly few reports of the use of their diiron counterparts in metal mediated synthesis. However, recent studies by Gilbertson have demonstrated that these complexes may also have a rich and varied reactivity with potential applications in organic synthesis. For instance, $[Fe_2(CO)_6(\mu\text{-SPr}^n)\{\mu\text{-O=C(CH=CHCH}_3)\}]$ undergoes *exo*-selective Diels–Alder reactions with Danishefsky's diene (Scheme 1a) [7], stereo and regioselective [3 + 2] cycloaddition reactions with nitrones, to give the corresponding 4-isoxazolidenes (Scheme 1b) [8], and kinetic resolution in its reaction with enantiomerically pure nitrones, derived from proline, to give the expected bicyclic isoxazolidene as a single diastereoisomer (Scheme 1c) [9].

In the vast majority of binuclear complexes the acyl ligand acts as a three-electron donor, through oxygen and carbon. Recently however, an alternative binding mode has been identified in which the acyl acts as a five-electron donor through additional coordination of the α,β-double bond [10].

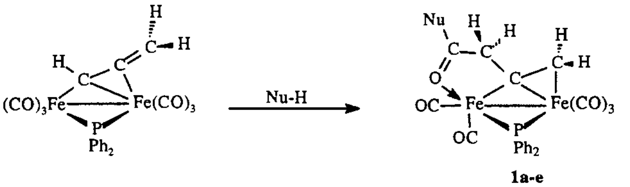

1a-e

(1)

We have recently been involved in a detailed study of the reactivity of the σ-η-allenyl ligand in $[Fe_2(CO)_6(\mu\text{-PPh}_2)\{\mu\text{-}\eta^1\text{:}\eta^2\text{-C(H)=C=CH}_2\}]$ towards a range of nucleophilic reagents [11], reasoning that the cumulated fragment $-CH=C=CH_2$ could be a potentially versatile building block for the synthesis of a wide range of organic products. Our studies have revealed that $[Fe_2(CO)_6(\mu\text{-PPh}_2)\{\mu\text{-}\eta^1\text{:}\eta^2\text{-C(H)=C=CH}_2\}]$ reacts with a range of amines and alcohols to give the β,γ-unsaturated amides and esters $[Fe_2(CO)_5(\mu\text{-PPh}_2)(\mu\text{ - }\eta^1(O)\text{:}\eta^1(C)\text{:}\eta^2(C)\text{-}\{NuC(O)CH_2\}C=CH_2\}]$ (**1a**–**e**), *via* a highly unusual nucleophile–carbonyl–allenyl coupling sequence (Eq. (1)) [12]. We became interested in the carbonyl insertion reactions of these complexes since the product of this transformation would be a highly functionalised α,β-unsaturated acyl, capable of binding to the metal centre through either the alkene or carbonyl group, and suitable for further functionalisation. Herein, we report that $[Fe_2(CO)_5(\mu\text{-PPh}_2)(\mu\text{-}\eta^1(O)\text{:}\eta^1(C)\text{:}\eta^2(C)\text{-}\{NuC(O)CH_2\}C=CH_2\}]$ reacts with dppm and dppe to give the corresponding phosphine substituted α,β-unsaturated acyl derivatives whereas trimethylphosphite reacts *via* carbonyl substitution to give the corresponding alkenyl derivatives (Scheme 2).

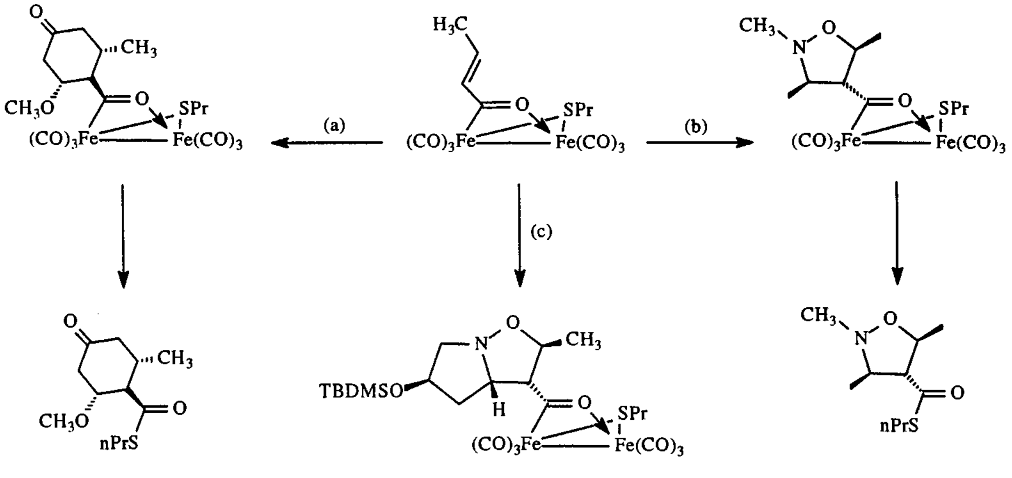

Scheme 1.

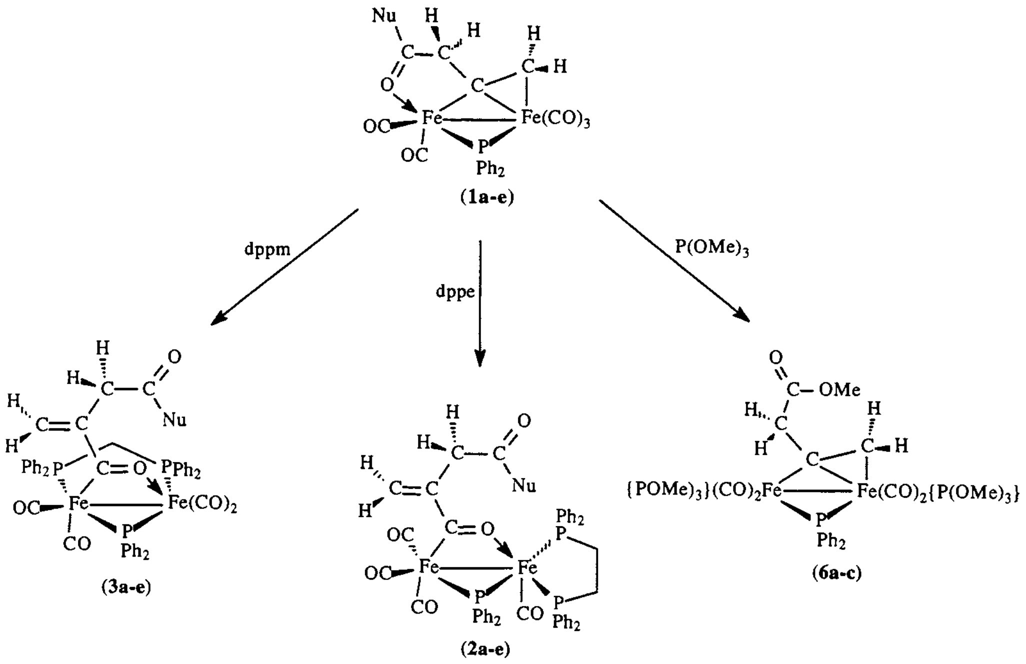

Scheme 2.

2. Experimental

2.1. General comments

Unless otherwise stated, all manipulations were carried out in an inert atmosphere glove box or by using standard Schlenk line techniques. Diethyl ether and hexane were distilled from Na–K alloy, tetrahydrofuran from potassium and dichloromethane from CaH$_2$. CDCl$_3$ was pre-dried with CaH$_2$ and vacuum transferred and stored over 4 Å molecular sieves. ^{1}H- and ^{31}P-NMR spectra were recorded on a JEOL LAMBDA 500 or Bruker AC 200, AMX 300 and DRX 500 machines. Column chromatography was carried out with alumina purchased from Aldrich Chemical Company and deactivated with 6% w/w water prior to loading. The diiron complexes [Fe$_2$(CO)$_6$(μ-PPh$_2$){μ-η^1:η^2-(H)C=C=CH$_2$}] [11c], [Fe$_2$(CO)$_5$(μ-PPh$_2$)(μ-η^1(C):η^2(C):η^1(O)–{Nu(O)CCH$_2$}C=CH$_2$)] (**1a**–**e**) [12a] and [Fe$_2$(CO)$_5${P(OMe)$_3$}(μ-PPh$_2$)(μ-η^1:η^2-{NuC(O)CH$_2$}C=CH$_2$}] (**4a**–**c**) [12b] were prepared as described previously.

*2.1.1. Synthesis of [Fe$_2$(CO)$_4$(μ-PPh$_2$)(η^2-dppe)-(μ-O=C–C{CH$_2$}–CH$_2$–C(O)OMe)] (**2a**)*

A diethyl ether solution of [Fe$_2$(CO)$_5$(μ-PPh$_2$)(μ-η^1(C):η^2(C):η^1(O)–{MeO(O)CCH$_2$}C=CH$_2$)] (**1a**) (0.200 g, 0.373 mmol) and dppe (0.746 mmol, 0.300 g) was stirred for 16 h. The solvent was then removed under reduced pressure and the residue dissolved in the minimum amount of dichloromethane (2–3 ml), absorbed onto deactivated alumina, desolvated and placed on a 300 × 30 mm^2 alumina column. Elution with an *n*-hexane–dichloromethane mixture (50:50, v/v) gave a single major band identified as **2a**. Crystallisation from dichloromethane–*n*-hexane gave **2a** as orange crystals in 65% yield (0.220 g). IR (ν(CO), cm^{-1}, C$_6$H$_{14}$): 2013 s, 1961 m, 1940 m, 1901 m, 1747 w, 1653 w. ^{31}P{^{1}H} (121.498 MHz, CDCl$_3$, δ): 167.9 (dd, $^2J_{PP}$ = 123.0 Hz, $^2J_{PP}$ = 11.0 Hz, μ-PPh$_2$), 85.9 (dd, $^2J_{PP}$ = 123.0 Hz, $^2J_{PP}$ = 23.1 Hz, dppe), 79.4 (dd, $^2J_{PP}$ = 23.1 Hz, $^2J_{PP}$ = 11.0 Hz, dppe). ^{1}H-NMR (200.132 MHz, CDCl$_3$, δ): 8.01–7.92 (m, 2H, C$_6$*H*$_5$), 7.38–6.76 (m, 26H, C$_6$*H*$_5$), 6.50–6.42 (m, 2H, C$_6$*H*$_5$), 6.19 (s, 1H, C=C*H*$_a$H$_b$), 5.63 (s, 1H, C=CH$_a$*H*$_b$), 3.51 (s, 3H, OC*H*$_3$), 3.16–2.78 (m, 2H, P–C*H*$_2$–CH$_2$–P), 2.66–2.31 (m, 2H, P–CH$_2$–C*H*$_2$–P), 2.13 (d, 1H, $^2J_{HH}$ = 16.5 Hz, (O)CC*H*$_c$H$_d$), 1.85 (d, 1H, $^2J_{HH}$ = 16.5 Hz, (O)CCH$_c$*H*$_d$). ^{13}C{^{1}H}-NMR (125.65 MHz, CDCl$_3$, δ): 288.7 (d, $^2J_{PC}$ = 16.6 Hz, μ-acyl), 218.1 (td, $^2J_{PC}$ = 12.6 Hz, $^2J_{PC}$ = 25.5 Hz, CO), 214.3 (m, CO), 172.0 (s, *C*(O)–OCH$_3$), 148.6 (s, *C*=CH$_2$), 140.9–127.3 (m, *C*$_6$H$_5$), 133.9 (d, $^4J_{PC}$ = 10.7 Hz, C=*C*H$_2$), 51.5 (s, O*C*H$_3$), 33.8 (s, *C*H$_2$–C(O)OCH$_3$), 31.6 (dd, $^1J_{PC}$ = 25.5 Hz, $^2J_{PC}$ = 15.4 Hz, P–*C*H$_2$–CH$_2$–P), 30.4 (ddd, $^1J_{PC}$ = 26.7 Hz, $^2J_{PC}$ = 14.2 Hz, $^3J_{PC}$ = 4.7 Hz P–CH$_2$–*C*H$_2$–P). Anal. Calc. for C$_{48}$H$_{41}$Fe$_2$O$_6$P$_3$: C, 61.70; H, 4.42. Found: C; 61.62; H, 4.28.

Compounds **2b**–**e** were prepared according to the procedure described above for **2a**.

*2.1.2. Synthesis of [Fe$_2$(CO)$_4$(μ-PPh$_2$)(η^2-dppe)-(μ-O=C–C{CH$_2$}–CH$_2$–C(O)OEt)] (**2b**)*

Isolated as dark red crystals in 65% yield from a dichloromethane solution layered with n-hexane at room temperature (r.t.). IR (ν(CO), cm^{-1}, C_6H_{14}): 2013 s, 1961 m, 1940 m, 1901 m, 1747 w, 1655 w. $^{31}P\{^1H\}$ (202.35 MHz, $CDCl_3$, δ): 168.1 (dd, $^2J_{PP} = 122.0$ Hz, $^2J_{PP} = 10.0$ Hz, μ-PPh$_2$), 85.8 (dd, $^2J_{PP} = 122.0$ Hz, $^2J_{PP} = 23.0$ Hz, dppe), 79.6 (dd, $^2J_{PP} = 23.0$ Hz, $^2J_{PP} = 10.0$ Hz, dppe). ^{1}H-NMR (500.0 MHz, $CDCl_3$, δ): 8.00–7.96 (m, 2H, C_6H_5), 7.43–6.79 (m, 26H, C_6H_5), 6.46 (m, 2H, C_6H_5), 6.18 (s, 1H, C=CH_aH$_b$), 5.63 (s, 1H, C=CH$_a$$H_b$), 4.01 (q, 2H, $^3J_{HH} = 6.8$ Hz, OCH_2CH$_3$), 3.02 (m, 2H, P–CH_2–CH$_2$–P), 2.48 (m, 2H, P–CH$_2$–CH_2–P), 2.13 (d, $^2J_{HH} = 14.5$ Hz, 1H, (O)CCH_cH$_d$), 1.87 (d, $^2J_{HH} = 14.5$ Hz, 1H, (O)CCH$_c$$H_d$), 1.18 (t, $^3J_{HH} = 6.8$ Hz, 3H, OCH$_2$CH_3). $^{13}C\{^1H\}$-NMR (125.65 MHz, $CDCl_3$, δ): 289.1 (br s, μ-acyl), 218.2 (br s, CO), 214.6 (m, CO), 171.7 (s, C(O)–OCH$_2$CH$_3$), 148.9 (s, C=CH$_2$), 140.6–127.4 (m, C$_6$$H_5$), 133.9 (d, $^4J_{PC} = 8.9$ Hz, C=CH$_2$), 60.3 (s, OCH$_2$CH$_3$), 34.1(s, CH$_2$–C(O)OEt), 31.5 (dd, $^1J_{PC} = 25.8$ Hz, $^2J_{PC} = 14.4$ Hz, P–CH$_2$–CH$_2$–P), 30.3 (ddd, $^1J_{PC} = 30.0$ Hz, $^2J_{PC} = 14.6$ Hz, $^3J_{PC} = 5.3$ Hz, P–CH$_2$–CH$_2$–P), 14.2 (s, OCH$_2$$CH_3$). Anal. Calc. for $C_{49}H_{43}Fe_2O_6P_3$: C, 62.05; H, 4.57. Found: C; 61.73; H, 4.42.

2.1.3. *Synthesis of* [$Fe_2(CO)_4(\mu\text{-}PPh_2)(\eta^2\text{-dppe})$-($\mu$-O=C–C{CH$_2$}–CH$_2$–C(O)OPr^i)] (**2c**)

Isolated as dark red crystals in 60% yield from a dichloromethane solution layered with *n*-hexane at r.t. IR (ν(CO), cm^{-1}, C_6H_{14}): 2013 s, 1961 m, 1940 m, 1903 w. $^{31}P\{^1H\}$ (121.498 MHz, $CDCl_3$, δ): 167.8 (dd, $^2J_{PP} = 122.2$ Hz, $^2J_{PP} = 10.6$ Hz, μ-PPh$_2$), 85.3 (dd, $^2J_{PP} = 122.2$ Hz, $^2J_{PP} = 23.1$ Hz, dppe), 79.5 (dd, $^2J_{PP} = 23.1$ Hz, $^2J_{PP} = 10.6$ Hz, dppe). ^{1}H-NMR (500.0 MHz, $CDCl_3$, δ): 8.00–7.96 (m, 2H, C_6H_5), 7.43–6.79 (m, 26H, C_6H_5), 6.48–6.14 (m, 2H, C_6H_5), 6.15 (s, 1H, C=CH_aH$_b$), 5.62 (s, 1H, C=CH$_a$$H_b$), 4.89 (sept, 1H, $^3J_{HH} = 6.4$ Hz, CH–(CH$_3$)$_2$), 3.03 (m, 2H, P–CH_2–CH$_2$–P), 2.47 (m, 2H, P–CH$_2$–CH_2–P), 2.10 (d, $^2J_{HH} = 15.9$ Hz, 1H, (O)CCH_cH$_d$), 1.87 (d, $^2J_{HH} = 15.9$ Hz, 1H, (O)CCH$_c$$H_d$), 1.61 (d, $^3J_{HH} = 6.4$ Hz, 6H, CH–(CH_3)$_2$). $^{13}C\{^1H\}$-NMR (125.65 MHz, $CDCl_3$, δ): 288.2 (d, $^2J_{PC} = 16.7$ Hz, μ-acyl), 218.4 (td, $^2J_{PC} = 29.0$ Hz, $^3J_{PC} = 16.7$ Hz, CO), 214.6 (m, CO), 171.2 (s, C(O)–CH$_3$), 149.1 (s, C=CH$_2$), 140.9–127.3 (m, C_6H$_5$), 133.9 (d, $^4J_{PC} = 9.6$ Hz, C=CH$_2$), 67.6 (s, CH–(CH$_3$)$_2$), 34.6 (s, CH$_2$–C(O)OPr^i), 31.5 (dd, $^1J_{PC} = 25.4$ Hz, $^2J_{PC} = 15.9$ Hz, P–CH$_2$–CH$_2$–P), 30.4 (ddd, $^1J_{PC} = 27.6$ Hz, $^2J_{PC} = 13.8$ Hz, $^3J_{PC} = 5.8$ Hz, P–CH$_2$–CH$_2$–P), 21.9 (s, CH–(CH$_3$)$_2$). Anal. Calc. for $C_{50}H_{45}Fe_2O_6P_3$: C, 62.39; H, 4.71. Found: C; 62.24; H, 4.49.

2.1.4. *Synthesis of* [$Fe_2(CO)_4(\mu\text{-}PPh_2)(\eta^2\text{-dppe})$-($\mu$-O=C–C{CH$_2$}–CH$_2$–C(O)NHPh)] (**2d**)

Isolated as dark red crystals in 65% yield from a dichloromethane solution layered with *n*-hexane at r.t. IR (ν(CO), cm^{-1}, C_6H_{14}): 2013 s, 1959 m, 1940 m, 1903 w. $^{31}P\{^1H\}$ (121.498 MHz, $CDCl_3$, δ): 168.6 (dd, $^2J_{PP} = 123.0$ Hz, $^2J_{PP} = 10.5$ Hz, μ-PPh$_2$), 84.5 (dd, $^2J_{PP} = 123.0$ Hz, $^2J_{PP} = 23.5$ Hz, dppe), 79.0 (dd, $^2J_{PP} = 23.5$ Hz, $^2J_{PP} = 10.5$ Hz, dppe). ^{1}H-NMR (500.0 MHz, $CDCl_3$, δ): 7.99–6.80 (m, 33H, C_6H_5), 6.56 (t, $^3J_{HH} = 8.8$ Hz, 2H, C_6H_5), 6.32 (s, 1H, NH), 6.19 (s, 1H, C=CH_aH$_b$), 5.75 (s, 1H, C=CH$_a$$H_b$), 3.18–2.82 (m, 2H, P–C$H_2$–CH$_2$–P), 2.61–2.38 (m, 2H, P–CH$_2$–CH_2–P), 2.17 (d, $^2J_{HH} = 15.8$ Hz, 1H, (O)CCH_cH$_d$), 1.99 (d, $^2J_{HH} = 15.8$ Hz, 1H, (O)CCH$_c$$H_d$). $^{13}C\{^1H\}$-NMR (125.65 MHz, $CDCl_3$, δ): 290.6 (br s, μ-acyl), 217.9 (br s, CO), 214.5 (m, CO), 168.5 (s, C(O)–NHPh), 149.9 (s, C=CH$_2$), 140.7–119.3 (m, C_6H$_5$), 133.9 (d, $^4J_{PC} = 8.0$ Hz, C=CH$_2$), 38.4 (s, CH$_2$C(O)), 31.7 (dd, $^1J_{PC} = 23.9$ Hz, $^2J_{PC} = 15.2$ Hz, P–CH$_2$–CH$_2$–P), 30.4 (m, P–CH$_2$–CH$_2$–P). Anal. Calc. for $C_{53}H_{44}Fe_2NO_6P_3$: C, 63.94; H, 4.45; N, 1.41. Found: C; 63.76; H, 4.61; N, 1.36.

2.1.5. *Synthesis of* [$Fe_2(CO)_4(\mu\text{-}PPh_2)(\eta^2\text{-dppe})$-($\mu$-O=C$_\alpha$–C$_\beta${C$_\gamma$H$_2$}–C$_\delta$H$_2$–C$_\varepsilon$(O)NHBu^t)] (**2e**)

Isolated as dark red crystals in 55% yield from a dichloromethane solution layered with *n*-hexane at r.t. IR (ν(CO), cm^{-1}, C_6H_{14}): 2013 s, 1959 m, 1938 m, 1903 w, 1722 w, 1691 w. $^{31}P\{^1H\}$ (121.498 MHz, $CDCl_3$, δ): 167.9 (dd, $^2J_{PP} = 123.8$ Hz, $^2J_{PP} = 11.1$ Hz, μ-PPh$_2$), 87.3 (dd, $^2J_{PP} = 123.8$ Hz, $^2J_{PP} = 23.7$ Hz, dppe), 79.1 (dd, $^2J_{PP} = 23.7$ Hz, $^2J_{PP} = 11.1$ Hz, dppe). ^{1}H-NMR (500.0 MHz, $CDCl_3$, δ): 7.98–6.54 (m, 30H, C_6H_5), 6.09 (s, 1H, C=CH_aH$_b$), 5.58 (s, 1H, C=CH$_a$$H_b$), 4.60 (s, 1H, N$H$), 3.07–2.91 (m, 2H, P–C$H_2$–CH$_2$–P), 2.59–2.50 (m, 2H, P–CH$_2$–CH_2–P), 1.76 (d, $^2J_{HH} = 16.5$ Hz, 1H, (O)CCH_cH$_d$), 1.61 (d, $^2J_{HH} = 16.5$ Hz, 1H, (O)CCH$_c$$H_d$), 1.23 (s, 9H, NHC(C$H_3$)$_3$). $^{13}C\{^1H\}$-NMR (125.65 MHz, $CDCl_3$, δ): 290.3 (d, $^2J_{PC} = 18.8$ Hz, μ-acyl), 218.2 (dt, $^2J_{PC} = 13.8$ Hz, $^2J_{PC} = 26.2$ Hz, CO), 214.3 (m, CO), 170.7 (s, C(O)–NHBu^t), 150.9 (s, C=CH$_2$), 140.6–127.2 (m, C_6H$_5$), 133.9 (d, $^4J_{PC} = 9.4$ Hz, C=CH$_2$), 51.1 (s, NHC(CH_3)$_3$), 38.4 (s, CH$_2$–C(O)NHBu^t), 31.9 (dd, $^1J_{PC} = 24.8$ Hz, $^2J_{PC} = 16.0$ Hz, P–CH$_2$–CH$_2$–P), 30.7 (ddd, $^1J_{PC} = 27.6$ Hz, $^2J_{PC} = 14.6$ Hz, $^3J_{PC} = 5.9$ Hz, P–CH$_2$–CH$_2$–P), 28.7 (s, NHC(CH$_3$)$_3$). Anal. Calc. for $C_{45}H_{48}Fe_2NO_6P_3$: C, 62.79; H, 4.96; N, 1.44. Found: C; 62.58; H, 4.87; N, 1.75.

2.1.6. *Synthesis of* [$Fe_2(CO)_4(\mu\text{-}PPh_2)(\mu\text{-dppm})$-($\mu$-O=C–C{CH$_2$}–CH$_2$–C(O)OMe)] (**3a**)

A toluene solution of [$Fe_2(CO)_5(\mu\text{-}PPh_2)(\mu\text{-}\eta^1(C)\text{:}\eta^2(C)\text{:}\eta^1(O)$–{MeO(O)CCH$_2$}C=CH$_2$)] (**1a**) (0.200 g, 0.373 mmol) and dppm (0.286 g, 0.746 mmol) was heated at 75°C for 3 h, after which time the solvent was removed to give a dark oily residue. This was dissolved in dichloromethane, absorbed onto deactivated alumina and desolvated under high vacuum, placed on a 300×30 mm^2 alumina column and eluted with *n*-hexane–dichloromethane (50/50, v/v) to give a major red–orange band which was crystallized from dichloromethane–*n*-hexane to give **4a** as orange crystals in 75% yield (0.257 g). IR (ν(CO), cm^{-1}, C_6H_{14}): 1990 m, 1957 s, 1923 m, 1911 m, 1739 w,. ^{31}P{^{1}H} (121.498 MHz, $CDCl_3$, δ): 209.9 (dd, $^{2}J_{PP} = 54.7$ Hz, $^{2}J_{PP} = 110.8$ Hz, μ-PPh_2), 53.2 (dd, $^{2}J_{PP} = 54.7$ Hz, $^{2}J_{PP} = 60.0$ Hz, dppm), 44.1 (dd, $^{2}J_{PP} = 110.8$ Hz, $^{2}J_{PP} = 60.0$ Hz, dppm). ^{1}H-NMR (200.132 MHz, $CDCl_3$, δ): 7.68–6.88 (m, 30H, C_6H_5), 5.09 (s, 1H, C=CH_aH$_b$), 5.01 (s, 1H, C=CH$_a$$H_b$), 3.47 (ddd, $^{2}J_{PH} = 23.8$ Hz, $^{2}J_{PH} = 13.4$ Hz, $^{2}J_{HH} = 3.3$ Hz, 1H, P–CH*H*–P), 2.88 (m, 1H, P–C*H*H–P), 2.86 (s, 3H, OCH_3), 2.03 (d, $^{2}J_{HH} = 16.8$ Hz, 1H, (O)CCH_cH$_d$), 1.92 (d, $^{2}J_{HH} = 16.8$ Hz, 1H, (O)CCH$_c$$H_d$). ^{13}C{^{1}H}-NMR (125.65 MHz, $CDCl_3$, δ): 301.2 (td, $^{2}J_{PC} = 21.5$ Hz, $^{3}J_{PC} = 3.6$ Hz, μ-acyl), 219.7 (t, $^{2}J_{PC} = 22.5$ Hz, CO), 218.2 (t, $^{2}J_{PC} = 19.0$ Hz, CO), 217.4 (s, *C*O), 213.4 (s, CO), 171.5 (s, *C*(O)–OCH_3), 147.6 (s, *C*=CH_2), 141.4–127.6 (m, *C*$_6$H$_5$), 133.3 (d, $^{4}J_{PC} = 8.3$ Hz, C=*C*H$_2$), 51.1 (s, O*C*H$_3$), 35.4 (m, C_δHH–C(O)OCH$_3$ and P–*C*H$_2$–P). Anal. Calc. for $C_{47}H_{39}Fe_2O_7P_3$: C, 61.33; H, 4.27. Found: C; 61.08; H, 4.39.

Compounds **3b**–**d** were prepared using a procedure similar to that described above for **3a**.

2.1.7. Synthesis of [$Fe_2(CO)_4$(μ-PPh_2)(μ-dppm)(μ-O=C–C{CH_2}–CH_2–C(O)OEt)] (3b)

Isolated as orange–red crystals in 75% yield from a dichloromethane solution layered with *n*-hexane at r.t. IR (ν(CO), cm^{-1}, C_6H_{14}): 1990 m, 1957 s, 1923 m, 1911 w. ^{31}P{^{1}H} (121.498 MHz, $CDCl_3$, δ): 210.1 (dd, $^{2}J_{PP} = 55.3$ Hz, $^{2}J_{PP} = 110.8$ Hz, μ-PPh_2), 53.4 (dd, $^{2}J_{PP} = 55.3$ Hz, $^{2}J_{PP} = 59.6$ Hz, dppm), 44.1 (dd, $^{2}J_{PP} = 110.8$ Hz, $^{2}J_{PP} = 59.6$ Hz, dppm). ^{1}H-NMR (500.0 MHz, $CDCl_3$, δ): 7.85–6.86 (m, 30H, C_6H_5), 5.09 (s, 1H, C=CH_aH$_b$), 4.99 (s, 1H, C=CH$_a$$H_b$), 3.47 (ddd, $^{2}J_{PH} = 26.8$ Hz, $^{2}J_{PH} = 13.2$ Hz, $^{2}J_{HH} = 3.1$ Hz, 1H, P–CH*H*–P), 3.23 (m, 2H, O*C*H$_2$CH$_3$), 2.89 (m, 1H, P–C*H*H–P), 2.02 (d, 1H, $^{2}J_{HH} = 16.8$ Hz, (O)CCH_cH$_d$), 1.91 (d, 1H, $^{2}J_{HH} = 16.8$ Hz, (O)CCH$_c$$H_d$), 0.82 (t, $^{3}J_{HH} = 5.5$ Hz, OCH$_2$CH_3). ^{13}C{^{1}H}-NMR (125.65 MHz, $CDCl_3$, δ): 301.4 (td, $^{2}J_{PC} = 22.2$ Hz, $^{3}J_{PC} = 3.6$ Hz, μ-acyl), 219.8 (t, $^{2}J_{PC} = 21.6$ Hz, CO), 218.2 (t, $^{2}J_{PC} = 19.6$ Hz, CO), 217.4 (s, *C*O), 213.4 (s, *C*O), 171.1 (s, C_ε(O)–OCH$_2$CH$_3$), 147.8 (s, *C*=CH$_2$), 141.4–127.6 (m, C$_6$H$_5$), 133.3 (d, $^{4}J_{PC} = 8.3$ Hz, C=*C*H$_2$), 59.9 (s, O*C*H$_2$CH$_3$), 35.5–35.3 (m, *C*H$_2$–C(O) and P–*C*H$_2$–P), 13.9 (s, OCH$_2$*C*H$_3$). Anal. Calc. for $C_{48}H_{41}Fe_2O_7P_3 \cdot 0.5CH_2Cl_2$: C, 59.63; H, 4.33. Found: C; 59.49; H, 4.27.

2.1.8. Synthesis of [$Fe_2(CO)_4$(μ-PPh_2)(μ-dppm)(μ-O=C–C{CH_2}–CH_2–C(O)OPr^i)] (3c)

Isolated as deep orange crystals in 70% yield from a dichloromethane solution layered with *n*-hexane at r.t. IR (ν(CO), cm^{-1}, C_6H_{14}): 1990 m, 1957 s, 1921 m, 1911 w. ^{31}P{^{1}H} (121.498 MHz, $CDCl_3$, δ): 210.0 (dd, $^{2}J_{PP} = 55.2$ Hz, $^{2}J_{PP} = 110.7$ Hz, μ-PPh_2), 53.0 (dd, $^{2}J_{PP} = 55.2$ Hz, $^{2}J_{PP} = 60.4$ Hz, dppm), 43.8 (dd, $^{2}J_{PP} = 110.7$ Hz, $^{2}J_{PP} = 60.4$ Hz, dppm). ^{1}H-NMR (500.0 MHz, $CDCl_3$, δ): 7.85–6.86 (m, 30H, C_6H_5), 5.09 (s, 1H, C=CH_aH$_b$), 4.97 (s, 1H, C=CH$_a$$H_b$), 4.18 (sept, $^{3}J_{HH} = 6.4$ Hz, 1H, C*H*–(CH$_3$)$_2$), 3.49 (ddd, $^{2}J_{PH} = 23.5$, $^{2}J_{PH} = 13.4$, $^{2}J_{HH} = 3.0$, 1H, P–CH_2–P), 2.89 (m, 1H, P–CH_2–P), 2.00 (d, $^{2}J_{HH} = 16.8$ Hz, 1H, (O)CCH_cH$_d$), 1.82 (d, $^{2}J_{HH} = 16.8$ Hz, 1H, (O)CCH$_c$$H_d$), 0.89 (d, $^{3}J_{HH} = 6.1$ Hz, 3H, CH(CH_3)CH$_3$), 0.78 (d, $^{3}J_{HH} = 6.1$ Hz, 3H, CH(CH$_3$)CH_3). ^{13}C{^{1}H} NMR (125.65 MHz, $CDCl_3$, δ): 301.4 (td, $^{2}J_{PC} = 21.0$ Hz, $^{3}J_{PC} =$ Hz, μ-*C*O), 219.8 (t, $^{2}J_{PC} = 24.0$ Hz, *C*O), 218.3 (t, $^{2}J_{PC} = 18.5$ Hz, *C*O), 217.5 (s, *C*O), 213.3 (s, *C*O), 170.8 (s, C_ε(O)–OPr^i), 148.2 (s, C_β=CH$_2$), 141.4–127.6 (m, *C*$_6$H$_5$), 133.3 (d, $^{4}J_{PC} = 7.6$ Hz, C=C_γH$_2$), 67.2 (s, *C*H(CH$_3$)$_2$), 35.6 (m, C_δHH–C(O)OPr^i and P–*C*H$_2$–P), 21.7 (s, CH(*C*H$_3$)CH$_3$), 21.5 (s, CH(CH$_3$)*C*H$_3$). Anal. Calc. for $C_{49}H_{43}Fe_2O_7P_3$: C, 62.05; H, 4.57. Found: C; 62.37; H, 5.08.

2.1.9. Synthesis of [$Fe_2(CO)_4$(μ-PPh_2)(μ-dppm)(μ-O=C–C{CH_2}–CH_2–C(O)NHPh)] (3d)

Prepared following the procedure used for **3a** except **1d** and dppm were heated in toluene at 85°C for 3 h. Isolated as orange–red crystals in 65% yield from a dichloromethane solution layered with *n*-hexane at r.t. IR (ν(CO), cm^{-1}, C_6H_{14}): 1990 s, 1957 s, 1921 m, 1912 w. ^{31}P{^{1}H} (121.498 MHz, $CDCl_3$, δ): 210.3 (dd, $^{2}J_{PP} = 54.1$ Hz, $^{2}J_{PP} = 111.2$ Hz, μ-PPh_2), 53.4 (dd, $^{2}J_{PP} = 54.1$ Hz, $^{2}J_{PP} = 60.6$ Hz, dppm), 44.1 (dd, $^{2}J_{PP} = 111.2$ Hz, $^{2}J_{PP} = 60.6$ Hz, dppm). ^{1}H-NMR (500.0 MHz, $CDCl_3$, δ): 7.91–6.78 (m, 35H, C_6H_5), 6.40 (s, 1H, N*H*), 5.17 (s, 1H, C=CH_aH$_b$), 5.07 (s, 1H, C=CH$_a$$H_b$), 3.57 (m, 1H, P–CH*H*–P), 2.84 (dd, $^{2}J_{PH} = 10.7$ Hz, $^{2}J_{PH} = 22.6$ Hz, 1H, P–CH_2–P), 1.90 (d, $^{2}J_{HH} = 15.9$ Hz, 1H, (O)CCH_cH$_d$), 1.83 (d, 1H, $^{2}J_{HH} = 15.0$ Hz, (O)CCH$_c$$H_d$). ^{13}C{^{1}H}-NMR (125.65 MHz, $CDCl_3$, δ): 303.9 (br t, $^{2}J_{PC} = 23.2$ Hz, μ-acyl), 219.3 (t, $^{2}J_{PC} = 23.2$ Hz, CO), 218.1 (t, $^{2}J_{PC} = 18.1$ Hz, CO), 217.5 (s, CO), 213.2 (s, CO), 168.3 (s, *C*(O)–NHPh), 149.0 (s, *C*=CH$_2$), 142.0–123.8 (m, *C*$_6$H$_5$), 133.3 (d, $^{4}J_{PC} = 8.0$ Hz, C=*C*H$_2$), 39.4 (m, *C*H$_2$–C(O) and P–*C*H$_2$–P). Anal. Calc. for $C_{52}H_{42}Fe_2NO_6P_3$:C, 63.63; H, 4.31; N, 1.43. Found: C; 63.67; H, 4.90; N, 1.40.

2.1.10. Synthesis of [$Fe_2(CO)_4${P(OMe)$_3$}(μ-PPh_2)(μ-η^1(C):η^2(C):η^1(O)–{MeO(O)CH$_2$}C=CH$_2$)] (5a)

Thermolysis of a toluene solution (20 ml) of [$Fe_2(CO)_5${P(OMe)$_3$}(μ-PPh_2)(μ-η^1:η^2-{MeO(O)CH$_2$}-C=CH$_2$)] (**4a**) (0.200 g, 0.303 mmol) for 6 h resulted in a gradual darkening of the solution. Removal of the volatiles gave a dark red solid which was chromatographed on alumina, eluting with *n*-hexane–dichloromethane (60:40, v/v), to give a major band which afforded **5a** as deep red crystals in 70% yield (0.134 g) after crystallisation by slow diffusion of *n*-hexane into a concentrated dichloromethane solution. IR (ν(CO), cm^{-1}, C_6H_{14}): 2004 m, 1952 m, 1928 s, 1905 w, 1660 w. $^{31}P\{^1H\}$ (121.498 MHz, $CDCl_3$, δ): 184.4 (d, $^2J_{PP} = 122.6$ Hz, μ-PPh_2), 172.8 (d, $^2J_{PP} = 122.6$ Hz, $P(OMe)_3$). ^1H-NMR (500.0 MHz, $CDCl_3$, δ): 7.48–7.06 (m, 10H, C_6H_5), 3.96 (d, $^2J_{HH} = 20.3$ Hz, 1H, $CH_cH_dC(O)Me$), 3.70 (s, 3H, OCH_3), 3.50 (d, $^2J_{PH} = 11.0$ Hz, 9H,$P(OCH_3)_3$), 3.10 (dd, $^2J_{HH} = 21.7$ Hz, $^4J_{PH} = 2.7$ Hz, $CH_cH_dC(O)Me$), 2.80 (ddd, $^2J_{HH} = 2.4$ Hz, $^3J_{PH} = 8.3$ Hz, $^3J_{PH} = 11.3$ Hz, 1H, $C{=}CH_aH_b$), 2.20 (br t, $^3J_{PH}, = 7.4$ Hz, $C{=}CH_aH_b$). $^{13}C\{^1H\}$ NMR (125.7 MHz, $CDCl_3$, δ): 219.3 (dd, $^2J_{PC} = 15.0$ Hz, $^2J_{PC} = 39.0$ Hz, CO), 218.7 (dd, $^2J_{PC} = 21.0$ Hz, $^2J_{PC} = 23.0$ Hz, CO), 217.8 (d, $^2J_{PC} = 12.4$ Hz, CO), 215.1 (d, $^2J_{PC} = 14.4$ Hz, CO), 186.4 (s, $C(O)Me$), 168.3 (d, $^2J_{PC} = 28.9$ Hz, $C{=}CH_2$), 141.4–127.2 (m, C_6H_5), 62.8 (br t, $^2J_{PC} = {}^2J_{PC} = 8.0$ Hz, $C{=}CH_2$), 53.5 (s, OCH_3), 52.7 (s, $CH_2C(O)Me$), 51.9 (d, $^2J_{PC} = 5.2$ Hz, $P(OCH_3)_3$). Anal. Calc. for $C_{24}H_{26}Fe_2O_9P_2{\cdot}CH_2Cl_2$: C, 41.87; H, 3.94. Found: C, 42.03; H, 3.74.

Compounds **5b**–**c** were prepared according to the procedure described above for **5a**.

2.1.11. Synthesis of $[Fe_2(CO)_4\{P(OMe)_3\}(\mu\text{-}PPh_2)(\mu\text{-}\eta^1(C){:}\eta^2(C){:}\eta^1(O)\{EtO(O)CH_2\}C{=}CH_2)]$ (**5b**)

Isolated as red crystals in 67% yield by slow diffusion of *n*-hexane into a dichloromethane solution. IR (ν(CO), cm^{-1}, C_6H_{14}): 2004 m, 1952 m, 1927 s, 1907 w, 1653 w. $^{31}P\{^1H\}$ (121.498 MHz, $CDCl_3$, δ): 184.5 (d, $^2J_{PP} = 120.0$ Hz, μ-PPh_2), 172.5 (d, $^2J_{PP} = 120.0$ Hz, $P(OMe)_3$). ^1H-NMR (500.0 MHz, $CDCl_3$, δ): 7.45–7.08 (m, 10H, C_6H_5), 4.13 (br d, $^3J_{HH} = 27.2$ Hz, 2H, OCH_2CH_3), 3.95 (br d, $^2J_{HH} = 21.4$ Hz, 1H, $CH_cH_dC(O)Me$), 3.51 (br d, $^2J_{PH} = 8.5$ Hz, 9H, $P(OCH_3)_3$), 3.09 (br d, $^2J_{HH} = 21.4$ Hz, $CH_cH_dC(O)Me$), 2.80 (br s, $C{=}CH_aH_b$), 1.87 (br s, $C{=}CH_aH_b$), 1.20 (br s, 3H, OCH_2CH_3). $^{13}C\{^1H\}$-NMR (125.7 MHz, $CDCl_3$, δ): 219.1 (dd, $^2J_{PC} = 16.6$ Hz, $^2J_{PC} = 42.3$ Hz, CO), 218.6 (dd, $^2J_{PC} = 21.7$ Hz, $^2J_{PC} = 22.7$ Hz, CO), 218.1 (d, $^2J_{PC} = 10.4$ Hz, CO), 215.0 (d, $^2J_{PC} = 14.4$ Hz, CO), 186.1 (s, $C(O)Et$), 168.5 (d, $^2J_{PC} = 28.9$ Hz, $C{=}CH_2$), 141.5–127.2 (m, C_6H_5), 63.5 (s, OCH_2CH_3), 62.7 (s, $C{=}CH_2$), 52.9 (s, $CH_2C(O)Et$), 51.9 (d, $^2J_{PC} = 5.2$ Hz, $P(OCH_3)_3$), 13.9 (s, OCH_2CH_3). Anal. Calc. for $C_{25}H_{28}Fe_2O_9P_2.CH_2Cl_2$: C, 42.72; H, 4.14. Found: C, 43.04; H, 4.10.

2.1.12. Synthesis of $[Fe_2(CO)_4\{P(OMe)_3\}(\mu\text{-}PPh_2)(\mu\text{-}\eta^1(C){:}\eta^2(C){:}\eta^1(O)\{^iPrO(O)CH_2\}C{=}CH_2)]$ (**5c**)

Isolated as red crystals in 63% yield by slow diffusion of *n*-hexane into a dichloromethane solution. IR (ν(CO), cm^{-1}, C_6H_{14}): 2004 m, 1952 m, 1927 s, 1903 w, 1647 w. $^{31}P\{^1H\}$ (121.498 MHz, $CDCl_3$, δ): 184.6 (d, $^2J_{PP} = 113.2$ Hz, μ-PPh_2), 172.1 (d, $^2J_{PP} = 113.2$ Hz, $P(OMe)_3$). ^1H-NMR (500.0 MHz, $CDCl_3$, δ): 7.47–7.07 (m, 10H, C_6H_5), 4.96 (sept, $^3J_{HH} = 6.1$ Hz, 1H, $OCH(CH_3)_2$), 3.92 (d, $^2J_{HH} = 21.7$ Hz, 1H, $CH_cH_dC(O)^iPr$), 3.52 (d, $^2J_{PH} = 10.7$ Hz, 9H, $P(OCH_3)_3$), 3.06 (d, $^2J_{HH} = 21.7$ Hz, $CH_cH_dC(O)^iPr$), 2.80 (br t, $^3J_{PH} = {}^3J_{PH} = 9.8$ Hz, $C{=}CH_aH_b$), 2.20 (br t, $^3J_{PH} = {}^3J_{PH} =$ Hz, $C{=}CH_aH_b$), 1.20 (d, $^3J_{HH} = 6.5$ Hz, 3H, $OCH(CH_3)CH_3$), 1.16 (d, $^3J_{HH} = 6.5$ Hz, 3H, $OCH(CH_3)CH_3$) $^{13}C\{^1H\}$-NMR (125.7 MHz, $CDCl_3$, δ): 219.2 (dd, $^2J_{PC} = 7.8$ Hz, $^2J_{PC} = 44.4$ Hz, CO), 218.7 (dd, $^2J_{PC} = 20.7$ Hz, $^2J_{PC} = 23.7$ Hz, CO), 218.2 (d, $^2J_{PC} = 16.6$ Hz, CO), 214.9 (d, $^2J_{PC} = 18.6$ Hz, CO), 185.6 (s, $C(O)Pr^i$), 168.5 (s, $C{=}CH_2$), 141.7–127.2 (m, C_6H_5), 71.8 (s, $OCH(CH_3)_2$), 62.6 (s, $C{=}CH_2$), 53.3 (s, $CH_2C(O)Et$), 51.9 (br s, $P(OCH_3)_3$), 21.7 (s, $OCH(CH_3)CH_3$), 21.6 (s, $OCH(CH_3)CH_3$). Anal. Calc. for $C_{26}H_{30}Fe_2O_9P_2$: C, 47.30; H, 4.58. Found: C, 47.12; H, 4.55.

2.1.13. Synthesis of $[Fe_2(CO)_4(\mu\text{-}PPh_2)\{P(OMe)_3\}_2(\mu\text{-}\eta^1(C){:}\eta^2(C)\text{–}\{MeO(O)CCH_2\}C{=}CH_2)]$ (**6a**)

Heating a toluene solution (20 ml) of $[Fe_2(CO)_5(\mu\text{-}PPh_2)(\mu\text{-}\eta^1(C){:}\eta^2(C){:}\eta^1(O)\text{–}\{MeO(O)CCH_2\}C{=}CH_2)]$ (**1a**) (0.200 g, 0.373 mmol) and trimethyl phosphite (0.090 ml, 0.746 mmol) at 75°C for 3 h, resulted in a colour change from orange to deep red. The solvent was removed to give a red solid which was purified by column chromatography, eluting with, *n*-hexane/dichloromethane (40:60, v/v) to give **6a** as a single major band. Slow diffusion of *n*-hexane into a concentrated dichloromethane solution gave orange crystals of **6a** in 70% yield (0.200 g). IR (ν(CO), cm^{-1}, C_6H_{14}): 2004 s, 1963 s, 1932 s, 1915 w. $^{31}P\{^1H\}$ (121.498 MHz, $CDCl_3$, 273 K, δ): 183.4 (d, $^3J_{PP} = 39.1$ Hz $P(OMe)_3$, **6a$_1$**), 181.2 (d, $^2J_{PP} = 108.7$ Hz, $P(OMe)_3$, **6a$_1$**), 180.3 (d, $^2J_{PP} = 103.8$ Hz, $P(OMe)_3$, **6a$_2$**), 177.5 (t, $^2J_{PP} = {}^2J_{PP} = 103.8$ Hz, PPh_2, **6a$_2$**), 170.6 (d, $^2J_{PP} = 103.8$ Hz, $P(OMe)_3$, **6a$_2$**), 149.0 (dd, $^2J_{PP} = 108.7$, 39.1 Hz, PPh_2, **6a$_1$**). ^1H-NMR (500.0 MHz, $CDCl_3$, δ): 7.62–7.10 (m, 10H, C_6H_5), 4.19 (d, $^3J_{PH} = 11.9$ Hz, 1H, $(O)CCH_cH_d$), 3.59 (d, $^3J_{PH} = 11.0$ Hz, 18H, $P(OCH_3)_3$), 3.02 (br m, 1H, $C{=}CH_aH_b$), 2.84 (br m, 1H, $(O)CCH_cH_d$), 2.22 (s, 1H, $C{=}CH_aH_b$). Anal. Calc. for $C_{27}H_{35}Fe_2O_{12}P_3$: C, 42.89; H, 4.67. Found: C; 43.01; H, 4.39.

Compounds **6b**–**c** were prepared according to the procedure described above for **6a**.

2.1.14. Synthesis of $[Fe_2(CO)_4(\mu\text{-}PPh_2)\{P(OMe)_3\}_2(\mu\text{-}\eta^1(C){:}\eta^2(C)\text{–}\{EtO(O)CCH_2\}C{=}CH_2)]$ (**6b**)

Isolated as deep orange crystals in 65% yield by slow diffusion of methanol into a concentrated dichloromethane solution at r.t. IR (ν(CO), cm^{-1},

C_6H_{14}): 2004 s, 1963 s, 1932 s, 1915 w. $^{31}P\{^1H\}$ (121.498 MHz, $CDCl_3$, δ): 183.3 (br s, $P(OMe)_3$, major isomer), 180.7 (d, $^2J_{PP} = 76.4$ Hz, $P(OMe)_3$, major and minor isomers), 175.9 (br s, PPh_2, minor isomer), 170.9 (br s, $P(OMe)_3$, minor isomer), δ 148.4 (br s, PPh_2, major isomer). ^1H-NMR (500.0 MHz, $CDCl_3$, δ): 7.62–7.09 (br m, 10H, C_6H_5), 4.20 (d, $^3J_{PH} = 16.2$ Hz, 1H, $(O)CCH_cH_d$), 4.16–4.10 (m, 2H, OCH_2CH_3), 3.59 (d, $^3J_{PH} = 11.0$ Hz, 18H, $P(OCH_3)_3$), 3.05 (br m, 1H, $C{=}CH_aH_b$), 2.83 (br m, 1H, $(O)CCH_cH_d$), 2.30 (s, 1H, $C{=}CH_aH_b$), 1.29 (t, $^3J_{HH} = 7.0$ Hz, 3H, OCH_2CH_3).

2.1.15. Synthesis of $[Fe_2(CO)_4(\mu\text{-}PPh_2)\{P(OMe)_3\}_2(\mu\text{-}\eta^1(C){:}\eta^2(C)\text{–}\{^iPrO(O)CCH_2\}C{=}CH_2)]$ ***(6c)***

Isolated as orange crystals in 64% yield by slow diffusion of *n*-hexane into a concentrated dichloromethane solution. IR (ν(CO), cm^{-1}, C_6H_{14}): 2004 s, 1963 s, 1932 s, 1915 w. $^{31}P\{^1H\}$ (121.498 MHz, $CDCl_3$, δ): 183.3 (br s, $P(OMe)_3$, major isomer), 180.8 (br s, $P(OMe)_3$, major and minor isomers), 175.2 (br, s, μ-PPh_2, minor isomer), 170.9 (br s, $P(OMe)_3$, minor isomer), δ 147.3 (br s, μ-PPh_2, major isomer). ^1H-NMR (500.0 MHz, $CDCl_3$, δ): 7.83–7.09 (br m, 10H, C_6H_5), 4.94 (br m, 1H, $CH(CH_3)_2$), 4.15 (d, $^3J_{PH} = 13.1$ Hz, 1H, $(O)CCH_cH_d$), 3.59 (d, $^3J_{PH} = 11.0$ Hz, 18H, $P(OCH_3)_3$), 3.08 (br m, 1H, $C{=}CH_aH_b$), 2.82 (br m, 1H, $(O)CCH_cH_d$), 2.26 (s, 1H, $C{=}CH_aH_b$), 1.28 (d, $^3J_{HH} = 6.1$ Hz, 3H, $CH(CH_3)_2$), 1.23 (d, $^3J_{HH} = 6.1$ Hz, 3H, $CH(CH_3)_2$).

2.2. X-ray crystallographic studies

All measurements were made on a Bruker AXS SMART CCD area-detector diffractometer, at 160 K, using graphite-monochromated Mo–K_α radiation ($\lambda = 0.71073$ Å) and narrow frame exposures (0.3° in ω). Cell parameters were refined from the observed ω angles of all strong reflections in each data set. Intensities were corrected semiempirically for absorption based on symmetry-equivalent and repeated reflections. The structures were solved by direct methods and refined on F^2 values for all unique data by full-matrix least squares. Table 1 gives further details. All non-hydrogen atoms were refined anisotropically. H-atoms, located in difference maps, were constrained with a riding model except for those attached to C(1) and C(3) in **5a**, and C(1) in **6a**, which had their coordinates refined freely because of non-standard geometry; U(H) was set to 1.2 (1.5 for methyl groups) times U_{eq} for the parent atom. Highly disordered CH_2Cl_2 solvent, estimated as half a molecule per molecule of complex **3a**, was treated by the SQUEEZE option of PLATON [13a]. Other programs used were Bruker AXS SMART and SAINT for diffractometer control and frame integration [13b], Bruker SHELXTL for structure solution, refinement and molecular graphics [13c], and local programs.

Table 1
Summary of crystal data and structure determination for compounds **2a**, **3a**, **5a** and **6a**

Compound	**2a**	**3a**·0.5CH_2Cl_2	**5a**	**6a**
Formula	$C_{48}H_{41}Fe_2O_7P_3$	$C_{47}H_{39}Fe_2O_7P_3.0.5CH_2Cl_2$	$C_{25}H_{28}Cl_2Fe_2O_9P_2$	$C_{27}H_{35}Fe_2O_{12}P_3$
M_r	934.4	962.9	717.0	756.2
Temperature (K)	160	173	160	160
Crystal system	Monoclinic	Orthorhombic	Monoclinic	Monoclinic
Space group	$C2/c$	$Pbcn$	$P2_1/n$	$P2_1/c$
a (Å)	44.912(2)	11.7295(14)	8.7969(5)	20.4629(14)
b (Å)	11.3227(5)	24.299(3)	20.1332(11)	9.7074(6)
c (Å)	17.9056(8)	31.701(4)	17.1050(9)	17.8652(12)
β (°)	110.746(2)		98.168(1)	113.783(2)
V (Å^3)	8515.1(7)	9035.4(18)	2998.7(3)	3247.4(4)
Z	8	8	4	4
μ (mm^{-1})	0.85	0.86	1.30	1.10
θ_{max} (°)	28.8	28.9	28.8	28.8
Reflections measured	26256	55092	18828	19540
Unique reflections	10 022	11 108	7087	7672
Reflections with $F^2 > 2\sigma(F^2)$	7507	8495	5164	6303
R_{int} (on F^2)	0.0479	0.0560	0.0446	0.0292
No. of parameters	542	533	405	411
R [a] $[I > 2\sigma(I)]$	0.0479	0.0560	0.0375	0.0354
wR [b] (all data)	0.1103	0.1197	0.0874	0.0948
GOF [c] (S)	1.043	1.109	0.965	1.098
Max, min diff map (e Å^{-3})	0.93, −0.61	0.48, −0.56	0.59, −0.71	0.52, −0.31

[a] Conventional $R = \Sigma||F_o| - |F_c||/\Sigma|F_o|$ for 'observed' reflections having $F_o^2 > 2\sigma(F_o^2)$.

[b] $wR = [\Sigma(F_o^2 - F_c^2)^2/\Sigma w(F_o^2)^2]^{1/2}$ for all data.

[c] $GOF = [\Sigma w(F_o^2 - F_c^2)^2/(\text{no. unique reflections} - \text{no. of parameters})]^{1/2}$.

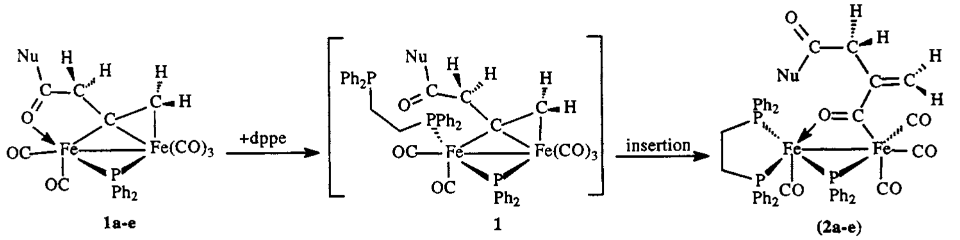

Scheme 3.

3. Results and discussion

3.1. Migratory insertion reactions: synthesis and characterisation of bridging acyl complexes

Thermolysis of a toluene solution of $[Fe_2(CO)_5(\mu\text{-}PPh_2)(\mu\text{ - }\eta^1(O):\eta^1(C):\eta^2(C)\text{-}\{NuC(O)CH_2\}C{=}CH_2)]$ (**1a**–**e**) and 1,2-bis(diphenylphosphino)ethane (dppe) results in carbonyl migration and formation of acyl-bridged $[Fe_2(CO)_4(\eta^2\text{-dppe})(\mu\text{-}PPh_2)(\mu\text{-}C{=}O\{C{=}CH_2\}\text{-}CH_2C(O)Nu)]$ (**2a**–**e**), as the sole products. The reaction is conveniently monitored by TLC and IR spectroscopy, with the appearance of a new $\nu(C{=}O)$ band at 1560 cm^{-1} typical of a carbonyl absorption of a bridging acyl ligand. Complexes **2a**–**e** were purified by column chromatography and characterised by ^1H-, $^{31}P\{^1H\}$- and $^{13}C\{^1H\}$-NMR spectroscopy and in the case of **2a** single-crystal X-ray crystallography. The ^1H-NMR spectra of **2a**–**e** contain four distinct sets of resonances, two doublets in the region δ 1.6–2.2 with a geminal coupling constant of ca. 16 Hz, corresponding to the diastereotopic methylene protons adjacent to the ester/amide carbonyl, and two singlets in the region δ 5.6–6.2 associated with the vinyl portion of the acyl bridge. The $^{31}P\{^1H\}$-NMR spectrum of **2a** contains a low-field doublet of doublets at δ 167.9 ($^2J_{PP} = 123.0$ Hz, $^2J_{PP} = 11.0$ Hz) and further doublets of doublets at δ 85.9 ($^2J_{PP} = 123.0$, 23.1Hz) and 79.4 ($^2J_{PP} = 23.1$, 11.0 Hz). The magnitude of the phosphorus–phosphorus coupling constants is a firm indication that the dppe acts in a *cis* chelating fashion with one phosphorus *cis* and the other *trans* to the phosphido-bridge [14]. In the $^{13}C\{^1H\}$-NMR spectrum, a low-field signal at δ 288.7 corresponds to the acyl carbon and is in the region characteristic of a μ-acyl bridging ligand [15]. Addition of dppe to **1a**–**e** is expected to result in displacement of the coordinated ester carbonyl, as has previously been observed with trimethylphosphite [12] (vide infra), followed by an intramolecular phosphine promoted carbonyl migration to give **2a**–**e** (Scheme 3). A $^{31}P\{^1H\}$-NMR spectrum of a toluene solution of **1a** and a slight excess of dppe, recorded before heating, contained three distinct well-separated signals, a low-field doublet at δ 173.1 ($^2J_{PP} = 113.2$ Hz), for the phosphido bridge, a doublet of doublets at δ 42.1 ($^2J_{PP} = 113.2$, 34.1 Hz) and a high-field doublet at δ -18.1 ($^2J_{PP} = 34.1$ Hz), which most likely correspond to the coordinated and uncoordinated phosphorus centres of the η^1-dppe complex **I**, respectively. Thermolysis of this mixture resulted in smooth conversion to the μ-acyl complex **2a**.

Under similar conditions **1a**–**d** react with dppm via loss of CO and 1,2-migratory insertion to give the corresponding dppm-acyl-bridged derivatives $[Fe_2(CO)_4(\mu\text{ - dppm})(\mu\text{ - }PPh_2)(\mu\text{ - }C{=}O\{C{=}CH_2\}CH_2C\text{-}(O)R)]$ (**3a**–**d**). The ^1H- and $^{13}C\{^1H\}$-NMR spectra are qualitatively similar to those of **2a**–**d**. For instance, the $^{31}P\{^1H\}$-NMR spectrum of **3a** contains a low-field doublet of doublets at δ 209.9 ($^2J_{PP} = 110.8$, 54.7 Hz) and high-field doublets of doublets at δ 53.2 ($^2J_{PP} = 54.7$, 60.0 Hz) and 44.1 ($^2J_{PP} = 110.8$, 60.0 Hz), which correspond to the phosphido group and the inequivalent ends of the dppm, respectively. The magnitude of the phosphorus–phosphorus coupling constants suggests a *trans* arrangement of the bridging phosphido group and dppm. Although both *cis* and *trans* arrangements of the phosphorus containing ligands in dppm-phosphido bridged diiron complexes are possible [14], the most common stereochemistry appears to be that in which the phosphorus ligands adopt a *trans* arrangement. In the case of **1a** in which the ester coordinated carbonyl occupies a site *trans* to the phosphido-bridge the formation of **3a** can be most aptly considered as a carbonyl displacement reaction with retention of stereochemistry at iron, presumably via an η^1-dppm intermediate.

Full structural details of the bridging acyl ligand and the mode of coordination of the diphosphine were provided by single-crystal X-ray analyses of **2a** and **3a**. Perspective views of the molecular structures of **2a** and **3a**, together with the atomic numbering scheme, are illustrated in Figs. 1 and 2, respectively, and a selection of bond lengths and angles for both compounds is listed in Table 2. The two iron atoms in **2a** are separated by a distance of 2.6928(5) Å and bridged asymmetrically by a phosphido ligand [Fe(1)–P(3) = 2.2393(8) Å; Fe(2)–P(3) = 2.2091(7) Å] and a 3-electron donor α,β-unsaturated acyl ligand, oxygen bound to Fe(2) [Fe(2)–O(1) = 1.9820(17) Å] and carbon bound to Fe(1) [Fe(1)–C(1) = 1.955(2) Å]. The acyl C(1)–O(1) bond length of 1.266(2) Å is similar to previously reported values [6b,17,18] and longer than a typical conjugated C–O double bond. The remaining carbon–carbon bonds within the bridging acyl ligand [C(2)–C(3) = 1.330(4) Å and C(2)–C(4) = 1.515(4) Å, C(4)–C(5) 1.494(4) Å] are consistent with localised double and single bonds. These carbon–carbon and carbon–oxygen bond lengths are similar to values reported previously in related α,β-unsaturated acyl complexes such as $[Fe_2(CO)_4(\mu\text{-PPh}_2)(\mu\text{-dppm})(\mu\text{-O=C–C(Ph)=CHPh})]$ [6h], $[Fe_2(CO)_6(\mu\text{-SBu}^t)(\mu\text{-O=C–C(OEt)=CH}_2)]$ [6b] and $[Fe_2(CO)_4(\mu\text{-dppm})(\mu\text{-PCy}_2)(\mu\text{-O=C–C(Ph)=CH}_2)]$ [17]. In a number of cases the bond length pattern in α,β-unsaturated acyl complexes is best described as delocalised to account for the near equal lengths of the carbon–carbon bonds [6,11i]. In a typical example, the two carbon–carbon bonds in the α,β-unsaturated acyl bridge in $[Fe_2(CO)_5\{P(OMe)_3\}(\mu\text{-PPh}_2)\{\mu\text{-O=C–CH=CMe(NHR)}\}]$ ($R = {}^i\text{Pr}$, CH_2Ph) [11i] are of similar length and the carbon–nitrogen bond length is in the region characteristic of an iminium salt. This bond length equivalence is most likely due to the presence of an amino group at the three-position which forms an extended delocalised system. The dppe coordinates in a chelating manner with one arm binding *trans* [P(1)–Fe(2)–P(2) = 161.18(3)°] and the other *cis* [P(2)–Fe(2)–P(2) = 110.71(3)°] to the phosphido-bridge, consistent with the J_{PP} couplings of 123.0 and 11.0 Hz, respectively. The bridging acyl ligand is *cis* to the phosphido and the carbonyl C(1)–O(1) lies approximately parallel to the iron–iron bond, the largest deviation form the least squares mean plane containing Fe(1), Fe(2), C(1), O(1) being 0.031 Å. The core structural features of **2a** and **3a**, in particular the *cis* disposition of the phosphido-bridge and the acyl

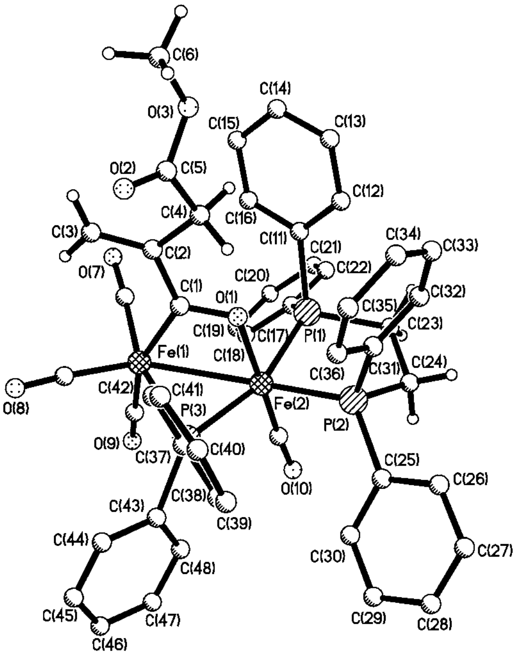

Fig. 1. Molecular structure of $[Fe_2(CO)_4(\eta^2\text{-dppe})(\mu\text{-PPh}_2)(\mu\text{-C=O}\{C=CH_2\}CH_2C(O)OMe)]$ (**2a**). Phenyl hydrogen atoms and the CH_2Cl_2 molecule of crystallisation have been omitted. Carbonyl carbons have the same numbers as oxygen atoms.

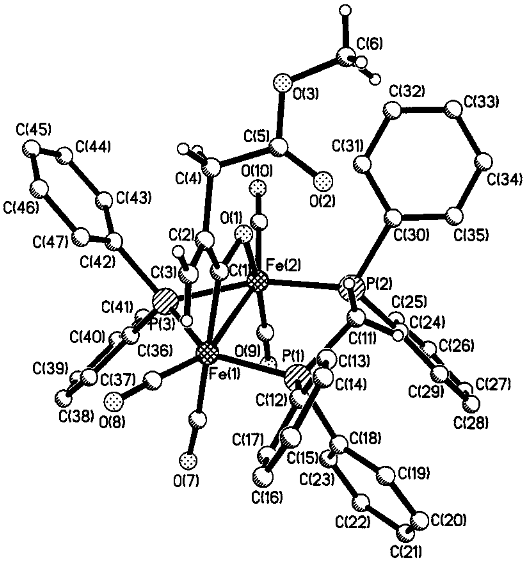

Fig. 2. Molecular structure of $[Fe_2(CO)_4(\mu\text{-dppm})(\mu\text{-PPh}_2)(\mu\text{-C=O}\{C=CH_2\}CH_2C(O)OMe)]$ (**3a**), Phenyl hydrogen atoms have been omitted. Carbonyl carbons have the same numbers as oxygen atoms.

Table 2
Selected bond lengths (Å) and bond angles (°) for **2a** and **3a**

2a		**3a**	
Bond lengths			
Fe(1)–Fe(2)	2.6928(5)	Fe(1)–Fe(2)	2.6394(5)
Fe(1)–P(3)	2.2393(8)	Fe(1)–P(3)	2.1950(8)
Fe(2)–P(3)	2.2091(7)	Fe(2)–P(3)	2.2026(8)
Fe(2)–P(1)	2.2350(7)	Fe(1)–P(1)	2.2222(8)
Fe(2)–P(2)	2.2086(8)	Fe(2)–P(2)	2.2596(8)
Fe(1)–C(1)	1.955(2)	Fe(1)–C(1)	1.952(3)
Fe(2)–O(1)	1.9820(17)	Fe(2)–O(1)	1.9915(17)
C(1)–O(1)	1.266(3)	C(1)–O(1)	1.274(3)
C(1)–C(2)	1.501(4)	C(1)–C(2)	1.494(4)
C(2)–C(3)	1.330(4)	C(2)–C(3)	1.326(4)
C(2)–C(4)	1.515(4)	C(2)–C(4)	1.510(3)
C(4)–C(5)	1.494(4)	C(4)–C(5)	1.495(4)
C(5)–O(2)	1.191(3)	C(5)–O(2)	1.197(4)
C(5)–O(3)	1.325(4)	C(5)–O(3)	1.351(3)
Bond angles			
Fe(1)–P(3)–Fe(2)	74.50(2)	Fe(1)–P(3)–Fe(2)	73.77(3)
P(3)–Fe(2)–P(2)	110.71(3)	P(3)–Fe(1)–P(1)	143.03(3)
P(3)–Fe(2)–P(1)	161.18(3)	P(3)–Fe(2)–P(2)	152.45(3)
P(3)–Fe(2)–C(10)	96.58(8)	O(1)–C(1)–C(2)	112.5(2)
O(1)–C(1)–C(2)	113.6(2)	C(1)–C(2)–C(3)	122.6(2)
C(1)–C(2)–C(3)	120.7(2)	C(1)–C(2)–C(4)	116.7(2)
C(4)–C(5)–O(3)	112.2(3)	C(4)–C(5)–O(3)	110.3(3)
C(4)–C(5)–O(2)	125.5(3)	C(4)–C(5)–O(2)	126.7(3)
O(2)–C(5)–O(3)	122.3(3)	O(2)–C(5)–O(3)	123.0(3)

group, the bond lengths and angles within the bridging hydrocarbyl ligand and the metal–metal and metal–phosphido are essentially the same. The most striking difference between the structures of **2a** and **3a** is a lengthening of the Fe–O bond from 1.9820(17) Å in **2a** to 1.9915(17) Å in **3a** ($\Delta = 0.0095$ Å). The molecular structure of **3a** clearly shows the *trans* arrangement of the phosphido-bridge and the diphosphine [P(3)–Fe(1)–P(1) = 143.03(3)°, P(3)–Fe(2)–P(2) = 152.45(3)°].

A number of binuclear complexes bridged by an α,β-unsaturated acyl ligand have appeared in the literature and in the vast majority of cases this ligand acts as a bridging three-electron donor by binding through the carbonyl oxygen and carbon atoms, in this regard **2a**–**e** and **3a**–**d** are unexceptional. The most straightforward route to α,β-unsaturated acyl complexes involves migratory insertion of CO into the σ-bond of a binuclear σ-η-alkenyl binuclear complex, although alternative methods have been developed and include: reaction of an acid chloride with $Na[Fe_2(CO)_6(\mu\text{-}PPh_2)]$ [6b], carbonylative amination of the multi-site bound acetylide $[Fe_2(CO)_6(\mu\text{-}PPh_2)(\mu\text{-}\eta^1\text{:}\eta^2\text{-}C{\equiv}CR)]$ [6g], carbonylation of the alkylidene bridged $[Fe_2(CO)_5\{P(OMe)_3\}(\mu\text{-}PPh_2)(\mu\text{-}CHCMe(NHR)\}]$ [11i] and reaction of $[NEt_3H][Fe_2(CO)_6(\mu\text{-}CO)(\mu\text{-}SR)]$ with alkynes or vinylmercuric halides [6c,d].

Seyferth has suggested that the stability of thiolate bridged α,β-unsaturated acyl (vinyl acyl) complexes of the type $[Fe_2(CO)_6(\mu\text{-}SR)(\mu\text{-}\eta^1\text{:}\eta^1\text{-}O{=}C{-}CH{=}CR^1R^2)]$ is related to the electron-donating ability of the substituted vinyl group attached to the bridging acyl carbon atom. The most stable α,β-unsaturated acyl complexes are those with two alkyl substituents on the C=C double bond, whereas those with only a single alkyl or aryl substituent attached to the β-carbon atom readily lose CO to afford the corresponding alkenyl bridged derivative, with first order kinetics. In contrast, phosphido-bridged α,β-unsaturated acyl complexes are, in general, more stable with respect to loss of CO. For instance, $[Fe_2(CO)_4(\mu\text{-}dppm)(\mu\text{-}PPh_2)\{\mu\text{-}O{=}C{-}C(Ph){=}CH_2\}]$ [6h] and $[Fe_2(CO)_5\{P(OMe)_3\}(\mu\text{-}PPh_2)(\mu\text{-}O{=}C{-}CH{=}CMe(NHR)\}]$ ($R = {}^iPr$, CH_2Ph) [11i] are both stable in refluxing toluene for prolonged periods, with no evidence for loss of CO. Similarly **3a**–**e** are stable under these conditions, with no evidence for decarbonlyation even after 12 h at reflux. Although we cannot yet provide a definitive explanation for the stability of **3a**–**e**, with respect to decarbonylation, it is tempting to suggest that the presence of a bulky substituent on the α-carbon atom is an important factor, as has previously been noted by Seyferth [6b–d].

3.2. Carbonyl substitution reactions

We have shown previously that trimethylphosphite readily displaces the metal-coordinated ester carbonyl in the β,γ-unsaturated esters and amides $[Fe_2(CO)_5(\mu\text{-}PPh_2)(\mu\text{-}\eta^1(O)\text{:}\eta^1(C)\text{:}\eta^2(C)\text{-}\{ROC(O)CH_2\}C{=}CH_2\}]$ (**1a**–**c**) to give the corresponding alkenyl complexes $[Fe_2(CO)_5\{P(OMe)_3\}(\mu\text{-}PPh_2)(\mu\text{-}\eta^1\text{:}\eta^2\text{-}\{ROC(O)CH_2\}\text{-}C{=}CH_2\}]$ (**4a**–**c**) [12]. The solid-state structure of $[Fe_2(CO)_5\{P(OMe)_3\}(\mu\text{-}PPh_2)(\mu\text{-}\eta^1\text{:}\eta^2\text{-}\{{}^iPrOC(O)CH_2\}\text{-}C{=}CH_2\}]$ (**4c**) showed that the trimethylphosphite occupies a site *trans* to the phosphido-bridge, revealing that the displacement occurs with retention of stereochemistry at iron. In an extension of these studies we have reacted **1a**–**c** with excess trimethylphosphite in an attempt to promote stepwise displacement and carbonyl migration to generate the corresponding phosphite substituted α,β-unsaturated acyl complexes. Heating toluene solutions of **1a**–**c** and trimethylphosphite results in substitution of the ester coordinated carbonyl to give $[Fe_2(CO)_5\{P(OMe)_3\}(\mu\text{-}PPh_2)(\mu\text{-}\eta^1\text{:}\eta^2\text{-}\{ROC(O)CH_2\}\text{-}C{=}CH_2\}]$ (**4a**–**c**) followed by carbonyl substitution to give the σ-η-alkenyl derivatives $[Fe_2(CO)_4\{P(OMe)_3\}_2\text{-}(\mu\text{-}PPh_2)(\mu\text{-:}\eta^1\text{:}\eta^2\text{-}\{ROC(O)CH_2\}C{=}CH_2\}]$ (**6a**–**c**). Notably, there was no evidence for migratory insertion to give the corresponding α,β-unsaturated acyl complexes.

In earlier work, Hogarth showed that thermolysis of a toluene solution of the α-phenyl ethenyl complex $[Fe_2(CO)_4(\mu\text{-}dppm)(\mu\text{-}PPh_2)(\mu\text{-}PhC{=}CH_2)]$ afforded three products, one of which was $[Fe_2(CO)_3(\mu\text{-}dppm)(\mu\text{-}PPh_2)\{\mu\text{-}O{=}C{-}C(Ph){=}CH_2\}]$, bridged by a five-elecron donor α,β-unsaturated acyl [10]. This prompted us to examine the thermal stability of $[Fe_2(CO)_5\{P(OMe)_3\}(\mu\text{-}PPh_2)(\mu\text{-}\eta^1\text{:}\eta^2\text{-}\{ROC(O)CH_2\}C{=}CH_2\}]$ (**4a**–**c**), specifically to examine its conversion into **6a**–**c** and/or possibility of promoting carbonyl migration to form similar five-electron donor acyl derivatives. Thermolysis of toluene solutions of **4a**–**c** resulted in loss of CO and coordination of the ester carbonyl to form complexes $[Fe_2(CO)_4\{P(OMe)_3\}(\mu\text{-}PPh_2)(\mu\text{-}\eta^1(O)\text{:}\eta^1(C)\text{:}\eta^2(C)\text{-}\{ROC(O)CH_2\}C{=}CH_2\}]$ (**5a**–**c**). Coordination of the ester carbonyl was clearly evident from the IR spectrum, which showed a shift of the carbonyl band from 1735 cm^{-1} in **4a** to 1660 cm^{-1} in **5a**. The $^{31}P\{^1H\}$-NMR spectrum of **5a** contains doublets at δ 184.4 and 172.8 ($^2J_{PP} = 122.6$ Hz), the magnitude of the coupling constant confirming a *trans* arrangement of the phosphorus containing ligands. The ^1H-NMR spectrum contains four multiplets associated with the hydrocarbyl bridge. The alkenyl protons appear as multiplets at δ 2.80 and 2.20 and the diastereotopic methylene protons as a doublet at δ 3.96 ($^2J_{HH} = 20.3$ Hz) and doublet of doublets at δ 3.10 ($^2J_{PP} = 20.3$, $^4J_{PH} = 2.7$ Hz). The ^{13}C signals associated with the μ-η^1:η^2-alkenyl ligand in **5a**–**c** appear in the region expected for such ligands and are similar to those in **1a**–**c**. Isolation of **5a**–**c** suggests that it is a likely intermediate in the formation of **6a**–**c** from **1a**–**b** and trimethylphosphite. Indeed, treatment of a deep red dichloromethane solution of **5a**–**c** with trimethylphosphite at room temperature results in

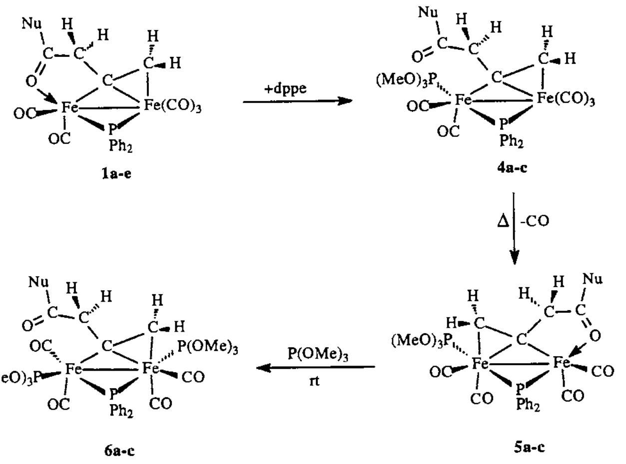

Scheme 4.

displacement of the ester coordinated carbonyl and quantitative conversion into orange–yellow **6a–c** within 10 min (Scheme 4). This transformation is most conveniently monitored by IR spectroscopy which clearly shows the disappearance of the band corresponding to the coordinated ester carbonyl (1660 cm^{-1}) and the appearance of a band due to the uncoordinated ester carbonyl (1730 cm^{-1}).

3.3. Variable temperature NMR studies

The room temperature $^{31}P\{^1H\}$-NMR spectrum of $[Fe_2(CO)_4\{P(OMe)_3\}_2(\mu\text{-}PPh_2)(\mu\text{-}C{=}O\{C{=}CH_2\}CH_2C(O)R)]$ (**6a**) contains a sharp doublet at δ 186.2 and several exchange broadened signals at δ 149, 170, 176 and 183. To investigate this exchange process further a variable temperature $^{31}P\{^1H\}$-NMR study was undertaken. The low temperature limiting spectrum of **6a** (Fig. 3) reveals two distinct sets of signals that correspond to a 60:40 mixture of two isomers in slow exchange, herein referred to as **6a$_1$** and **6a$_2$**, respectively [●, major isomer **6a$_1$**; ▽, minor isomer **6a$_2$**]. One set comprises a doublet of doublets at δ 149.0 ($^2J_{PP}$ = 108.7, 39.1 Hz) and two doublets at δ 183.4 ($^2J_{PP}$ = 39.1 Hz) and 181.2 ($^2J_{PP}$ = 108.7 Hz) and the other a triplet at δ 177.5 ($^2J_{PP}$ = $^2J_{PP}$ = 103.8 Hz) and two doublets at δ 170.6 ($^2J_{PP}$ = 103.8 Hz) and 180.3 ($^2J_{PP}$ = 103.8 Hz). The disparate magnitudes of the phosphorus–phosphorus coupling constants associated with the former set of resonances strongly suggests that one of the trimethylphosphites in this isomer, **6a$_1$**, is located *cis* to the phosphido bridge and the other *trans*, whereas the similarity in the phosphorus–phosphorus coupling constants in the latter set is consistent with both trimethylphosphites *trans* to the phosphido bridge, i.e. isomer **6a$_2$**. Clearly these two isomers are related by a

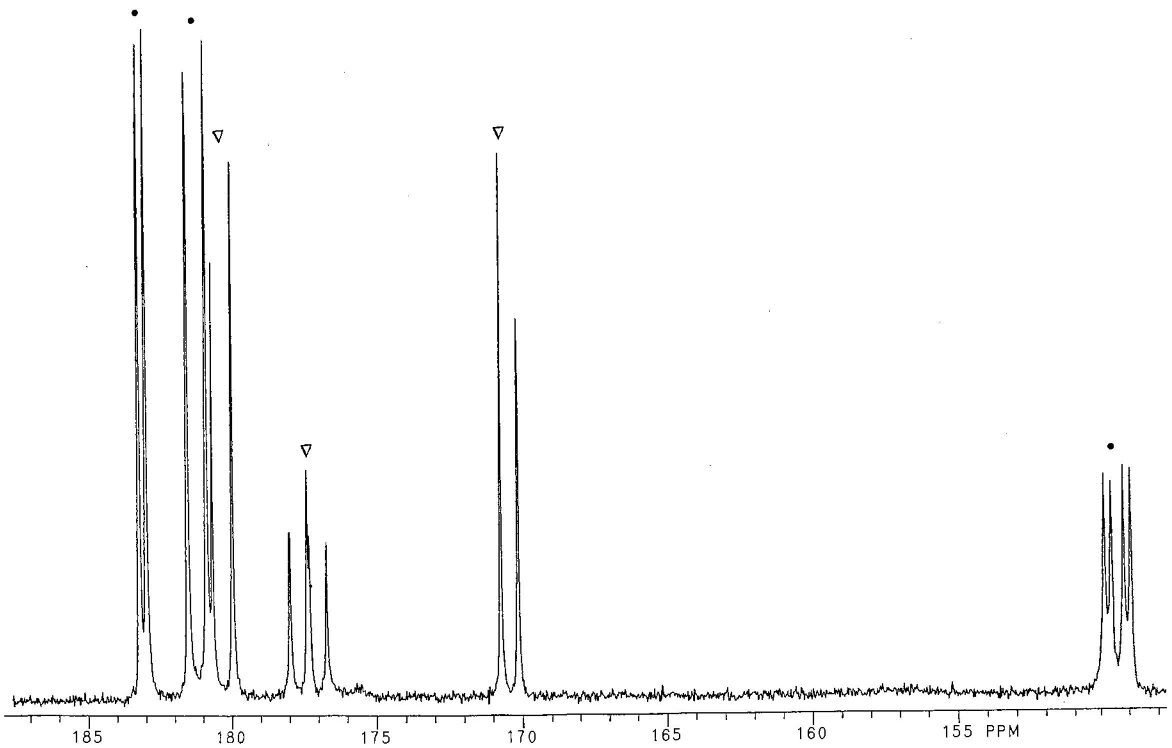

Fig. 3. Low temperature limiting $^{31}P\{^1H\}$-NMR spectrum of $[Fe_2(CO)_4\{P(OMe)_3\}_2(\mu\text{-}PPh_2)(\mu\text{-}C{=}O\{C{=}CH_2\}CH_2C(O)OMe)]$ (**6a**) recorded at 253 K showing the assignment of isomers **6a$_1$** and **6a$_2$** [●, isomer **6a$_1$** one P(OMe)$_3$ *trans* and one *cis* to PPh$_2$; ▽, isomer **6a$_2$** both P(OMe)$_3$ *trans* to PPh$_2$].

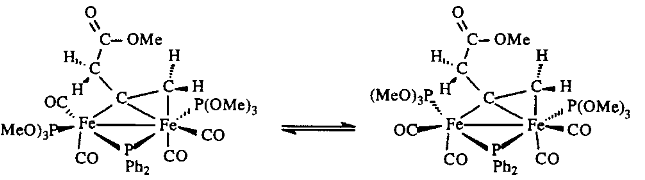

6a$_1$ **6a$_2$**

Scheme 5.

trigonal twist of one of the Fe(CO)$_2$P fragments (Scheme 5). As the temperature is raised the two signals at δ 181.2 and 180.3 rapidly coalesce and sharpen into a doublet at δ 180.9 ($^2J_{PP} = 76.8$ Hz) while the remaining resonances broaden over a much larger temperature range. At 253 K the signals belonging to the phosphido-bridges (δ 177.5 and 149.0) begin to exchange as do those associated with the remaining trimethylphosphites (δ 183.4 and 170.6). The temperature dependence of the ^{31}P{^{1}H}-NMR spectra clearly shows that above room temperature the two isomers interconvert rapidly.

Not surprisingly the room temperature ^{1}H-NMR spectrum of **6a** consists of four distinct resonances associated with protons of the bridging β,γ-unsaturated ester; doublets at δ 4.3 ($J = 14.7$ Hz) and 3.18 ($^2J_{PP} = 13.0$ Hz) a doublet of doublets at δ 2.95 ($^2J_{PP} = 8.0$, 14.0 Hz) and a broad unresolved triplet at δ 2.25. Variable temperature ^{1}H-NMR studies revealed that these signals broaden as the temperature is lowered and eventually sharpen to give rise to a set of eight near equal intensity resonances, fully consistent with the presence of two isomers in slow exchange.

Our interpretation of the variable temperature ^{31}P{^{1}H}-NMR studies has been supported by magnetisation transfer experiments (EXSY). An EXSY spectrum (Fig. 4), recorded at 278 K, clearly shows that the signals at δ 149.0 and 177.5, associated with the phosphido-bridges of the two isomers, exchange. This spectrum also shows that the signals at δ 183.4 and 181.2, which correspond to the trimethylphosphites of one isomer, exchange with those at δ 180.3 and 170.6, respectively, the trimethylphosphites in the other isomer. Exchange rates, extracted from the 2D intensity matrix using the programme D2DNMR, have been used to estimate the free energy of activation for this exchange process [19]. The rate of interconversion of **6a$_1$** to **6a$_2$** is approximately 22 s^{-1}, which equates to a free energy of activation for the process of 14.4 kcal mol^{-1}. The absence of exchange peaks between trimethylphosphites within an isomer clearly suggests that σ,η-alkenyl flipping is slow on the NMR timescale.

The spectroscopic characteristics described above and free energy of activation for this exchange are consistent with a dynamic process that involves interchange of isomer **6a$_1$** and **6a$_2$** via a restricted trigonal twist at one of the phosphite substituted iron centres. This process interchanges one isomer, with both trimethylphosphites *trans* to the phosphido bridge ($^2J_{PP} = 107.6$ Hz), with the other isomer, in which one phosphite occupies the site *trans* to the iron–iron bond ($^2J_{PP} = 39.1$ Hz), while the other occupies the site *trans* to the phosphido-bridge. The free energy of activation associated with the trigonal twist is close to the reported values of 15.0 kcal mol^{-1} for [Os$_3$(CO)$_{10}$-{P(OMe)$_3$}$_2$] and 13.8 kcal mol^{-1} for [Os$_3$(CO)$_9$-{P(OMe)$_3$}$_3$] [16] each of which is significantly higher than the values reported for [Fe$_2$(CO)$_5${P(OMe)$_3$}(μ-PPh$_2$){μ-C(H)CMe(NHPr^i)}] ($\Delta G^{\ddagger}$ = of 9.5 kcal mol^{-1}) and [Fe$_2$(CO)$_5${P(OMe)$_3$}(μ-PPh$_2$){μ-O=CCHC=CMe-(NHCH$_2$Ph)}] ($\Delta G^{\ddagger} = 10.4$ kcal mol^{-1}).

*3.4. X-ray crystal structures of [Fe$_2$(CO)$_4${P(OMe)$_3$}-(μ-PPh$_2$)(μ-η^1(O):η^1(C):η^2(C)–{MeOC(O)CH$_2$}-C=CH$_2$}] (**5a**) and [Fe$_2$(CO)$_4${P(OMe)$_3$}$_2$(μ-PPh$_2$)-(μ-:η^1:η^2-{MeOC(O)CH$_2$}C=CH$_2$}] (**6a**)*

A single-crystal X-ray study was carried out to determine the precise structural features of **5a**, the result of which is shown in Fig. 5, with selected bond lengths and angles listed in Table 3. The molecular structure confirms that the ester carbonyl oxygen coordinates to Fe(2) to form a five-membered metallacycle, such that O(1) is *trans* to P(2) [O(1)–Fe(2)–P(2) = 153.26(5)°], with Fe(2)–O(1) [2.0930(16) Å] and C(4)–O(1) [1.226(3) Å] bond lengths similar to those recently reported for [Fe$_2$(CO)$_4${η^2-C(CO$_2$Me)=CH(CO$_2$Me)=O}(μ-PPh$_2$)(μ-dppm)] [14a] and [Fe$_2$(CO)$_5$(μ-PPh$_2$)(μ-η^1:η^2-{^{i}PrOC(O)CH$_2$}C=CH$_2$}] [12b]. The remainder of the coordination sphere of Fe(2) is completed by the α-carbon atom of the bridging β,γ-unsaturated ester [Fe(2)–C(2) = 1.944(2) Å] and two carbonyls. The coordination geometry at Fe(1) is trigonal bipyramidal and consists of two carbonyls, trimethylphosphite, which occupies the site *trans* to the phosphido bridge [P(2)–Fe(1)–P(1) = 169.69(3)°], and the C(1)–C(2) bond [1.395(3) Å] of the alkenyl group [Fe(1)–C(1) = 2.169(2) Å, Fe(1)–C(2) = 2.117(2) Å].

A single-crystal X-ray analysis of **6a** was also undertaken, to provide full structural details of the bridging ligand and the positions of substitution of the phosphite ligands. The molecular structure is shown in Fig. 6 and a selection of bond lengths and angles is listed in Table 4. The molecular structure clearly shows two iron atoms separated by a distance of 2.6128(4) Å and bridged asymmetrically by a phosphido group [Fe(1)–P(3) = 2.2398(6) Å, Fe(2)–P(3) = 2.2225(6) Å] and a β,γ-unsaturated ester, σ-bonded to Fe(2) [Fe(2)–C(2) = 1.984(2) Å] and η^2-bonded to Fe(1) [Fe(1)–C(1)

2.154(2) Å; Fe(1)–C(2) = 2.118(2) Å]. The C(1)–C(2) bond length of 1.402(3) Å is comparable to values reported previously for binuclear alkenyl complexes [19] and is slightly longer than expected for a carbon–carbon double bond. The coordination sphere of both iron atoms is completed by two carbonyls and one trimethylphosphite. The trimethylphosphite located on Fe(1) is *trans* to the phosphido-bridge [P(3)–Fe(1)–P(1) = 178.72(3)°] while the other, attached to Fe(2), is *cis* to the phosphido bridge [P(2)–Fe(2)–P(3) = 99.40(2)°]. The alkenyl ligand adopts the familiar *endo* conformation with respect to the phosphido bridge [20], presumably to avoid unfavourable steric interactions between the substituents on C_α and the phenyl rings of the bridging phosphido group.

We have shown that diiron complexes bridged by α,β-unsaturated ester and amides react with bidentate phosphines via a pathway involving site selective displacement of the ester/amide coordinated carbonyl *trans* to the phosphido-bridge to give an η^1-dppe intermediate which then undergoes an intramolecular phosphine assisted migratory carbonyl insertion to afford the corresponding α,β-unsaturated ester/amide. In **2a–e** the dppe coordinates in a bidentate manner to

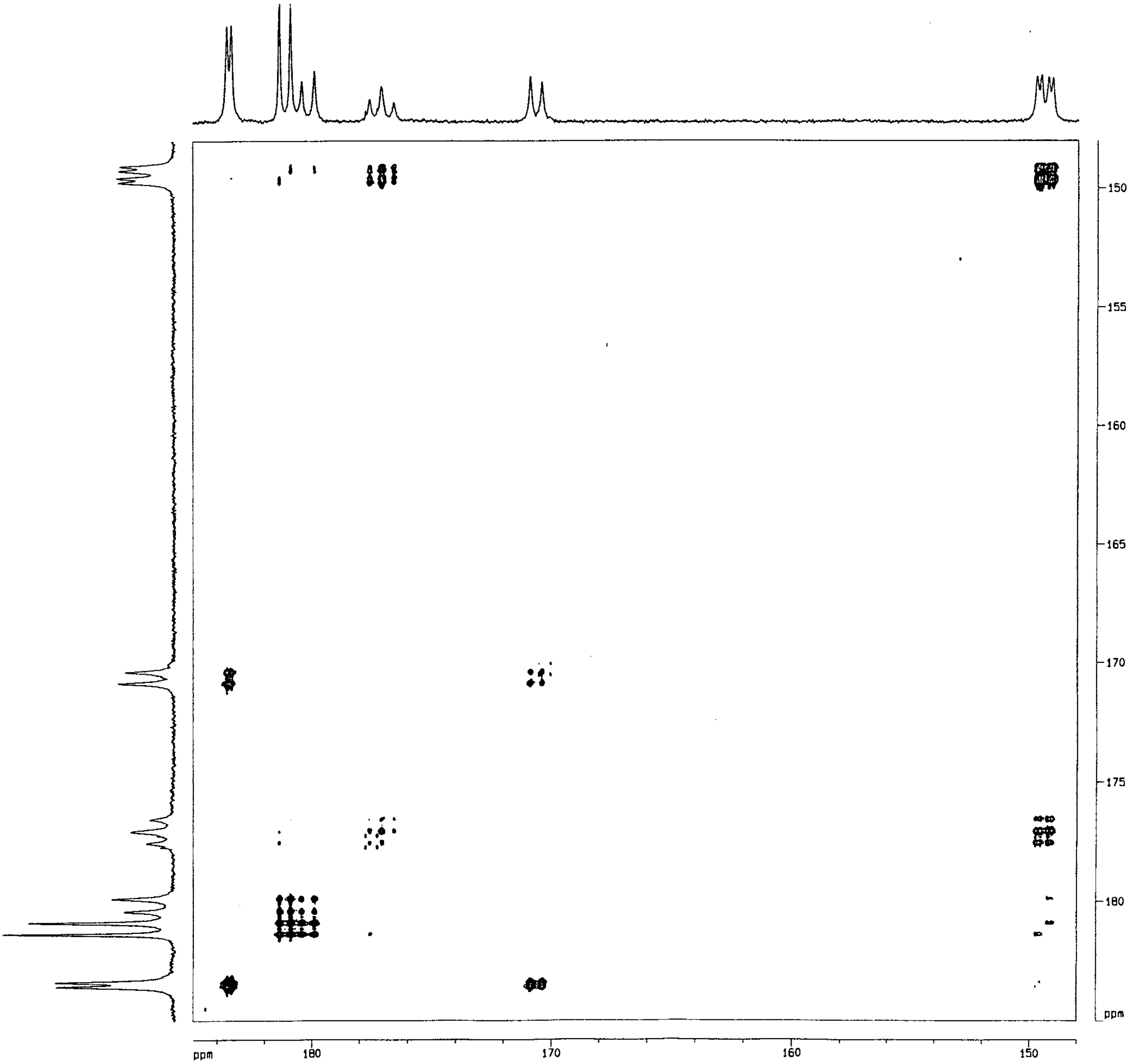

Fig. 4. ^{31}P-EXSY spectrum of [$Fe_2(CO)_4\{P(OMe)_3\}_2(\mu\text{-}PPh_2)(\mu\text{-}C{=}O\{C{=}CH_2\}CH_2C(O)OMe)$] (**6a**) recorded at 278 K, showing exchange of isomer of **6a$_1$** and **6a$_2$**.

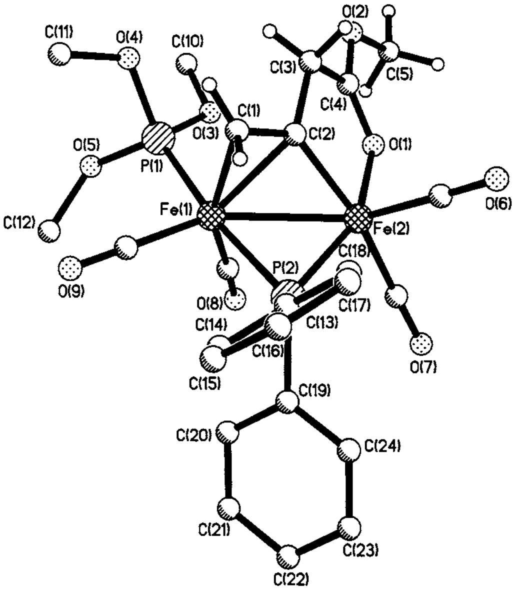

Fig. 5. Molecular structure of give $[Fe_2(CO)_4\{P(OMe)_3\}(\mu\text{-}PPh_2)(\mu\text{-}\eta^1(O):\eta^1(C):\eta^2(C)\text{–}\{NuC(O)CH_2\}C{=}CH_2\}]$ (**5a**). Phenyl and trimethylphosphite hydrogen atoms have been omitted. Carbonyl carbons have the same numbers as oxygen atoms.

Table 3
Selected bond lengths (Å) and bond angles (°) for **5a**

Bond lengths			
Fe(1)–Fe(2)	2.6076(5)	Fe(1)–P(2)	2.2310(7)
Fe(2)–P(2)	2.1707(7)	Fe(1)–P(1)	2.1602(7)
Fe(1)–C(1)	2.169(2)	Fe(1)–C(2)	2.117(2)
Fe(2)–C(2)	1.944(2)	Fe(2)–O(1)	2.0930(16)
Fe(2)–C(6)	1.747(3)	Fe(2)–C(7)	1.805(3)
Fe(1)–C(8)	1.755(3)	Fe(1)–C(9)	1.778(3)
C(1)–C(2)	1.395(3)	C(2)–C(3)	1.522(3)
C(3)–C(4)	1.489(3)	C(4)–O(1)	1.226(3)
C(4)–O(2)	1.319(3)		
Bond angles			
Fe(1)–P(2)–Fe(2)	72.64(2)	P(1)–Fe(1)–P(2)	169.69(3)
P(2)–Fe(2)–O(1)	153.26(5)	P(1)–Fe(1)–C(1)	96.49(7)
P(1)–Fe(1)–C(2)	93.20(7)	C(1)–C(2)–C(3)	117.7(2)
C(2)–C(3)–C(4)	108.9(2)	C(3)–C(4)–O(1)	121.0(2)
Fe(2)–O(1)–C(4)	112.82(15)	C(3)–C(4)–O(2)	115.4(2)
O(1)–C(4)–O(2)	123.6(2)		

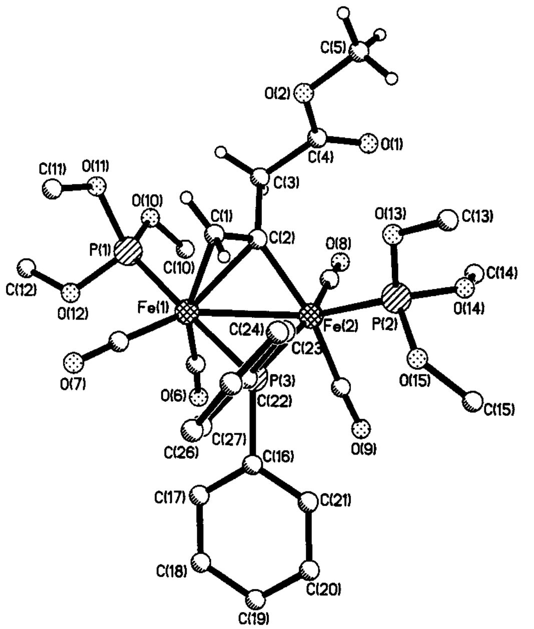

Fig. 6. Molecular structure of give $[Fe_2(CO)_4\{P(OMe)_3\}_2(\mu\text{-}PPh_2)(\mu\text{-}C{=}O\{C{=}CH_2\}CH_2C(O)OMe)]$ (**6a**). Phenyl and trimethylphosphite hydrogen atoms have been omitted. Carbonyl carbons have the same numbers as oxygen atoms.

Table 4
Selected bond lengths (Å) and bond angles (°) for **6a**

Bond lengths			
Fe(1)–Fe(2)	2.6128(4)	Fe(1)–P(3)	2.2398(6)
Fe(2)–P(3)	2.2225(6)	Fe(1)–P(1)	2.1716(6)
Fe(2)–P(2)	2.1412(7)	Fe(1)–C(1)	2.154(2)
Fe(1)–C(2)	2.118(2)	Fe(2)–C(2)	1.984(2)
C(1)–C(2)	1.402(3)	C(2)–C(3)	1.540(3)
C(3)–C(4)	1.507(3)	C(4)–O(1)	1.206(3)
C(4)–O(2)	1.343(3)		
Bond angles			
Fe(1)–P(3)–Fe(2)	71.68(2)	P(1)–Fe(1)–P(3)	178.72(3)
P(2)–Fe(2)–P(3)	99.40(2)	Fe(1)–Fe(2)–P(2)	138.26(2)
P(1)–Fe(1)–Fe(2)	125.05(2)	Fe(2)–C(2)–Fe(1)	79.06(7)
Fe(1)–C(1)–C(2)	69.47(12)	Fe(1)–C(2)–C(1)	72.22(12)
Fe(1)–C(2)–C(3)	123.63(15)	C(2)–C(3)–C(4)	109.55(19)
C(3)–C(4)–O(1)	125.8(2)	C(3)–C(4)–O(2)	111.2(2)
O(1)–C(4)–O(2)	123.0(2)		

the iron atom bound to the acyl oxygen, whereas in **3a**–**d** the dppm bridges the two metal atoms and is *trans* with respect to the phosphido–bridge. Under similar conditions **1a**–**c** react with trimethylphosphite to give $[Fe_2(CO)_4(\mu\text{-}PPh_2)\{P(OMe)_3\}_2(\mu\text{-}\eta^1(C):\eta^2(C)\text{–}\{RO(O)CCH_2\}C{=}CH_2)]$, most likely via a stepwise process involving displacement of the ester coordinated carbonyl, loss of carbon monoxide and reformation of the metallacycle ring and a subsequent displacement with a second molecule of trimethylphosphite. We have also shown that the α-functionalised alkenyl complex $[Fe_2(CO)_4(\mu\text{-}PPh_2)\{P(OMe)_3\}_2(\mu\text{-}\eta^1(C):\eta^2(C)\text{–}\{MeO(O)CCH_2\}C{=}CH_2)]$ (**6a**) exists as a mixture of two isomers that interconvert via a trigonal twist process, and that σ,η-exchange via the windshield wiper process is slow on the NMR timescale.

4. Supplementary material

Crystallographic data for the structural analysis have been deposited with the Cambridge Crystallographic Data Centre, CCDC nos. 148651 (**2a**), 148652 (**3a**), 148653 (**5a**), 148654 (**6a**). Copies of this information may be obtained free of charge from The Director, CCDC, 12 Union Road, Cambridge CB2 1EZ, UK (Fax: +44-1223-336033; e-mail deposit@ccdc.com.ac.uk or http://www.ccdc.cam.ac.uk).

Acknowledgements

We thank the University of Newcastle upon Tyne for financial support (S.D.) and the EPSRC for funding for a diffractometer (W.C.). We thank Dr A.E. Aliev (UCL) for help with EXSY experiments.

References

[1] J.P. Collman, L.S. Hegedus, J.R. Norton, R.G. Finke, Principles and Applications of Organotransition Metal Chemistry, University Science Books, Mill Valley, CA, 1987.

[2] (a) S.G. Davies Pure Appl. Chem. 60 (1988) 13. (b) K. Blacksurn, S.G. Davies K.H. Sutton, M. Whittaker, Chem. Soc. Rev. (1988) 1714. (c) G. Bashiardes, S.G. Davies, Tetrahedron Lett. 28 (1987) 5563. (d) R.P. Beckett, S.G. Davies, A.A Mortlock, Tetrahedron Asymmetry 3 (1992) 123.

[3] J. Tsuji, Transition Metal Reagents and Catalyst. Innovations in Organic Synthesis, Wiley, Chichester, 2000.

[4] (a) M. Brookhart, Y. Lou, E.W. Goldman, D.A. Timmers, G.D. Williams, J. Am. Chem. Soc. 113 (1991) 927. (b) M. Brookhart, W.B. Studabaker, Chem. Rev. 87 (1987) 411. (c) W. Petz, Iron–Carbene Complexes, Springer-Verlag, Berlin, 1993.

[5] (a) L. Cassar, A. Giarruso, Gazz. Chim. Ital. 103 (1973) 793. (b) M.C Baird, J.T. Mague, J.A. Osborn, G. Wilkinson, J. Chem. Soc. A. (1967) 1347. (c) H. Brix, W. Beck, J. Organomet. Chem. 234 (1982) 151. (d) D.L. Reger, L.J. Mintz, L.J. Lebioda, J. Am. Chem. Soc. 108 (1986) 1940. (e) D.L. Reger, S.A. Klaeren, J.E. Babin, R.D. Adams, Organometallics 7 (1988) 181.

[6] (a) D. Seyferth, K.S. Brewer, T.G. Wood, M. Cowie, R.W. Hilts, Organometallics 11 (1992) 2570. (b) D. Seyferth, J.B. Hoke, J.C. Dewan, P. Hofmann, M. Schnellbach, Organometallics 13 (1994) 3452. (c) D. Seyferth, C.M. Archer, D.P. Ruschke, M. Cowie, R.W. Hilts Organometallics 10 (1991) 3363. (d) D. Seyferth, J.B. Hoke, G.B. Womack, Organometallics 9 (1990) 2662. (e) D. Seyferth, J.B. Hoke, D.R. Wheeler, J. Organomet. Chem. 341 (1988) 421. (f) D. Seyferth, C.B. Womack, J.C. Dewan, Organometallics 4 (1985) 398. (g) G.N. Mott, R. Granby, S.A. MacLaughlin, N.J. Taylor, A.J. Carty, Organometallics 1 (1982) 189. (h) G. Hogarth, K. Shukri, S. Doherty, A.J. Carty, G.D. Enright, Inorg. Chim. Acta. 291 (1999) 178. (i) K. Henrick, J.A. Iggo, A.C. Kemball, M.J. Mays, P.R. Raithby, J. Chem. Soc. Dalton Trans. (1987) 2669.

[7] S.R. Gilbertson, X. Zhao, D.P. Dawson, K.L. Marshall, J. Am. Chem. Soc. 115 (1993) 8517.

[8] (a) S.R. Gilbertson, D.P. Dawson, O.D. Lopez, K.L. Marshall, J. Am. Chem. Soc. 117 (1995) 4431. (b) S.R. Gilbertson, O.D. Lopez, J. Am. Chem. Soc. 119 (1997) 3399.

[9] S.R. Gilbertson, O.D. Lopez, Angew. Chem. Int. Ed. Engl. 38 (1999) 1116.

[10] S. Doherty, G. Hogarth, Inorg. Chem. Commun. 1 (1998) 257.

[11] (a) S. Doherty, M. Waugh, T.S. Scanlan, M.R.J. Elsegood, W. Clegg, Organometallics 18 (1999) 679. (b) S. Doherty, J.F. Corrigan, A.J. Carty, E. Sappa, Adv. Organomet. Chem. 37 (1995) 39. (c) S. Doherty, M.R.J. Elsegood, W. Clegg, N.H. Rees, T.S. Scanlan, M. Waugh, Organometallics 16 (1997) 3221. (d) N. Carleton, J.F. Corrigan, S. Doherty, R. Pixner, Y. Sun, N.J. Taylor, A.J. Carty, Organometallics 13 (1994) 4179. (e) S. Doherty, G. Hogarth, M. Waugh, T.S. Scanlan, W. Clegg, M.R.J. Elsegood, Organometallics 18 (1999) 3178. (f) S. Doherty, M.R.J. Elsegood, W. Clegg, T.S. Scanlan, N.H. Rees, Chem. Commun. (1996) 1545. (g) S. Doherty, M.R.J. Elsegood, W. Clegg, M.F. Ward, M. Waugh, Organometallics 16 (1997) 4251. (h) S. Doherty, M.R.J. Elsegood, W. Clegg, D. Mampe, Organometallics 15, (1996) 5302. (i) S. Doherty, G. Hogarth, M.R.J. Elsegood, W. Clegg, N.H. Rees, M. Waugh, Organometallics 17 (1998) 3331.

[12] (a) S. Doherty, M.R.J. Elsegood, W. Clegg, M. Waugh, Organometallics 15 (1996) 2688. (b) S. Doherty, M.R.J. Elsegood, W. Clegg, D. Mampe, Organometallics 16 (1997) 1186.

[13] (a) A.L. Spek, PLATON, University of Utrecht, The Netherlands, 2000. (b) SMART and SAINT software for CCD diffractometers, Bruker AXS Inc., Madison, WI, 1994. (c) G.M. Sheldrick, SHELXTL user manual, version 5, Bruker AXS Inc., Madison, WI, 1994.

[14] (a) G. Hogarth, M.H. Lavender, J. Chem. Soc. Dalton Trans. (1994) 3389. (b) G. Hogarth, M.H. Lavender, J. Chem. Soc. Dalton Trans. (1992) 2759. (c) G. Hogarth, M.H. Lavender, K. Shukri, Organometallics 14 (1995) 2325. (d) D. Glushove, G. Hogarth, M.H. Lavender, J. Organomet. Chem. 528 (1997) 3.

[15] (a) Y.-F. Yu, J. Gallucci, A. Wojcicki, J. Am. Chem. Soc. 105 (1983) 4826. (b) R.P Rosen, J.B. Hoke, R.R. Whittle, G.L. Geoffroy, J.P. Hutchinson, J.A. Zubieta, Organometallics 3 (1984) 836.

[16] (a) J. Cooke, J. Takats, Organometallics 14 (1995) 698. (b) R.F. Alex, R.J. Pomeroy, Organometallics 6 (1987) 2437. (c) J. Cooke, R.E.D. McClung, J. Takats, R.D. Rogers, Organometallics 15 (1996) 4459.

[17] G. Hogarth, M.H. Lavender, K. Shukri, J. Organomet. Chem. 527 (1997) 247.

[18] Z. Xue, W.J. Seiber, C.B. Knobler, H.D. Kaesz, J. Am. Chem. Soc. 112 (1990) 1825.

[19] E.W. Abel, T.P.J. Coston, K.G. Orrell, V. Sik, D. Stephenson, J. Magn. Reson. 79 (1986) 34.

[20] S.A. MacLaughlin, S. Doherty, N.J. Taylor, A.C. Carty, Organometallics 11 (1992) 4315.